

000 001 002 003 004 005 006 007 008 009 010 011 ALPHAZEROES: DIRECT SCORE MAXIMIZATION CAN 012 OUTPERFORM PLANNING LOSS MINIMIZATION IN 013 SINGLE-AGENT SETTINGS 014 015 016 017 018 019 020 021 022 023 024 025 026 027 028

Anonymous authors

Paper under double-blind review

011 ABSTRACT 012

013 Planning at execution time has been shown to dramatically improve performance
014 for AI agents. A well-known family of approaches to planning at execution time
015 in single-agent settings and two-player zero-sum games are AlphaZero and its
016 variants, which use Monte Carlo tree search together with a neural network that
017 guides the search by predicting state values and action probabilities. AlphaZero
018 trains these networks by minimizing a planning loss that makes the value prediction
019 match the episode return, and the policy prediction at the root of the search tree
020 match the output of the full tree expansion. AlphaZero has been applied to various
021 single-agent environments that require careful planning, with great success. In this
022 paper, we explore an intriguing question: in single-agent settings, can we outper-
023 form AlphaZero by directly maximizing the episode score instead of minimizing
024 this planning loss, while leaving the MCTS algorithm and neural architecture
025 unchanged? To directly maximize the episode score, we use evolution strategies,
026 a family of algorithms for zeroth-order blackbox optimization. We compare both
027 approaches across multiple single-agent environments. Our experiments suggest
028 that directly maximizing the episode score tends to outperform minimizing the
029 planning loss.

030 031 032 1 INTRODUCTION 033

034
035 Lookahead search and reasoning is a central paradigm in artificial intelligence, and has a long
036 history (Newell and Ernst, 1965; Hart et al., 1968; Nilsson, 1971; Hart et al., 1972; Lanctot et al.,
037 2017; Brown et al., 2018). In many domains, planning at execution time significantly improves
038 performance. In domains like Sokoban, Pacman, and 2048, all state-of-the-art approaches use some
039 form of planning by the agent. Many planning approaches use *Monte Carlo Tree Search (MCTS)*,
040 which iteratively grows a search tree from the current state, and does so asymmetrically according to
041 the information seen so far. A prominent subfamily of approaches in this category are AlphaZero
042 and its variants, which leverage function approximation via neural networks to learn good heuristic
043 predictions of the values and action distributions at each state, which can be used to guide the tree
044 search. AlphaZero (and its variants) train this prediction function by minimizing a *planning loss*
045 consisting of the sum of a *value loss* and a *policy loss*.

046 In this paper, we set out to explore whether we can outperform AlphaZero and its variants in single-
047 agent environments by *directly maximizing the episode score* instead, while leaving all other aspects
048 of the agent, MCTS algorithm, and neural architecture unchanged. Since MCTS is not differentiable,
049 to maximize the episode score, we employ evolution strategies, a family of algorithms for zeroth-order
050 black-box optimization.

051 The structure of the paper is as follows. In §2, we present a detailed formulation of the problem. In
052 §3, we describe related work. In §4, we present our method. In §5, we describe our experimental
053 benchmarks and present our results. In §6, we discuss the experimental results. In §7, we present our
conclusion and suggest directions for future research.

054
055
056
057
058
059
060
061
062
063
064
065
066
067
068
069
070
071
072
073
074
075
076
077
078
079
080
081
082
083
084
085
086
087
088
089
090
091
092
093
094
095
096
097
098
099
0100
0101
0102
0103
0104
0105
0106
0107

2 PROBLEM FORMULATION

In this section, we formulate the problem in detail and introduce notation. If \mathcal{X} is a set, $\Delta\mathcal{X}$ denotes the set of probability distributions on \mathcal{X} . An *environment* is a tuple $(\mathcal{S}, \mathcal{A}, \rho, \delta)$ where \mathcal{S} is a set of states, \mathcal{A} is a set of actions, $\rho : \Delta\mathcal{S}$ is an initial state distribution, and $\delta : \mathcal{S} \times \mathcal{A} \rightarrow \mathbb{R} \times \mathbb{R} \times \mathcal{S}$ is a transition function. A *policy* is a function $\mathcal{S} \rightarrow \Delta\mathcal{A}$ that maps a state to an action distribution. Given an environment and policy, an *episode* is a tuple (s, a, r, γ) that is generated as follows. First, an initial state $s_0 \sim \rho$ is sampled. Thereafter, on each timestep $t \in \mathbb{N}$, an action $a_t \sim \pi(s_t)$ is sampled, and a reward, discount factor, and new state $(r_t, \gamma_t, s_{t+1}) = \delta(s_t, a_t)$ are obtained. The discount factor represents the probability of the episode ending at that timestep. For a given episode, the *return* at timestep $t \in \mathbb{N}$ is defined recursively as $R_t = r_t + \gamma_t R_{t+1}$. The *score* is the return at the initial timestep, R_0 . Our goal is to find a policy $\pi : \mathcal{S} \rightarrow \Delta\mathcal{A}$ that maximizes the expected score $\mathbb{E} R_0$.

3 RELATED WORK

In this section, we describe related work. Monte Carlo methods are a wide class of computational algorithms that use repeated random sampling to estimate numerical quantities. In the setting of planning, Monte-Carlo evaluation estimates the value of a position by averaging the return of several random rollouts. *Monte-Carlo Tree Search (MCTS)* (Coulom, 2007) combines Monte-Carlo evaluation with tree search. Instead of backing-up the min-max value close to the root, and the average value at some depth, it uses a more general backup operator that progressively changes from averaging to min-max as the number of simulations grows. MCTS grows the search tree asymmetrically, focusing on more promising subtrees.

AlphaGo (Silver et al., 2016) used a variant of MCTS to tackle the two-player board game of Go. It used a neural network to evaluate board positions *and* select moves. These networks are trained using a combination of supervised learning from human expert games and reinforcement learning from self-play. It was the first computer program to defeat a human professional player. AlphaGo Zero (Silver et al., 2017a) used reinforcement learning alone, *without* any human data, guidance or domain knowledge beyond game rules. AlphaZero (Silver et al., 2018) generalized AlphaGo Zero into a single algorithm that achieved superhuman performance in many challenging domains.

MuZero (Schrittwieser et al., 2020) combined AlphaZero’s tree-based search with a *learned dynamics model*. The latter allows it to plan in environments where the agent does *not* have access to a simulator of the environment at execution time. Gumbel MuZero (Danihelka et al., 2022) is a policy improvement algorithm based on sampling actions without replacement. It replaces the more heuristic mechanisms by which AlphaZero selects actions at root and non-root nodes. Empirically, it yields significantly better performance when planning with few simulations.

MCTS is a state-of-the-art general-purpose technique for search, planning, and optimization in single-agent settings. For example, in the papers that introduced them, the prominent MCTS-based methods MuZero and Gumbel MuZero were shown to be state of the art in single-agent settings, including 57 different Atari games, the canonical video game environment for testing AI techniques. Świechowski et al. (2023) note that “Automated planning is one of the major domains of application of the MCTS algorithm outside games.” Vallati et al. (2015) note that winning approaches of the International Probabilistic Planning Competition were using MCTS. This competition included combinatorial optimization problems, such as the minimization of open stacks problem (Yanasse and Senne, 2010).

MCTS has also been used in other discrete combinatorial problems, such as polynomial evaluation (Kuipers et al., 2013), low latency communication (Jia et al., 2020), generating large-scale floor plans with adjacency constraints (Shi et al., 2020), query selection in kidney exchange (McElfresh et al., 2020), and preference elicitation (Martin et al., 2024). Abe et al. (2019) used AlphaZero to solve NP-hard problems on graphs, including min vertex cover and max cut. Fawzi et al. (2022) used an AlphaZero-based algorithm, AlphaTensor, to discover efficient and provably-correct algorithms for multiplication of arbitrary matrices. Xu and Lieberherr (2019) showed that neural MCTS can be used in a general way to solve combinatorial optimization problems.

108 4 PROPOSED METHOD
109110 In this section, we present a detailed description of our proposed method, which we call AlphaZeroES.
111 The essential difference to AlphaZero is described in §4.3.
112113 4.1 PLANNING ALGORITHM
114115 We use the implementation of Gumbel MuZero (Danihelka et al., 2022), which is the prior state of the
116 art for this setting, found in the open-source Google DeepMind library Mctx (DeepMind et al., 2020).
117 It iteratively constructs a search tree starting from a state s_0 . Each node in the tree contains a state,
118 predicted value, predicted action probabilities, and, for each action, a visit count N , action value
119 Q , reward, and discount factor. Each iteration of the algorithm consists of three phases: *selection*,
120 *expansion*, and *backpropagation*.
121122 During *selection*, we start at the root and traverse the tree until a leaf edge is reached. At internal
123 nodes, we select actions according to the policy described in Danihelka et al. (2022). When we
124 reach a leaf edge (s, a) , we perform *expansion* as follows. We compute $(r, \gamma, s') = \delta(s, a)$, storing
125 r and γ in the edge’s parent node. We then query the agent’s *prediction function* $(v, p) = f_\theta(s')$ to
126 obtain the predicted value and action probabilities of s' . A new node is added to the tree containing
127 this information, with action visit counts and action values initialized to zero. Finally, we perform
128 *backpropagation* as follows. The new node’s value estimate is backpropagated up the tree to the root
129 in the form of an n -step return. Specifically, from $t = T$ to 0, where T is the length of the trajectory,
130 we compute an estimate of the cumulative discounted return G_t that bootstraps from the value
131 estimate v : $G_T = v$ and $G_t = r_t + \gamma_t G_{t+1}$. For each such t , we update the statistics for the edge
132 corresponding to (s_t, a_t) as follows: $Q(s_t, a_t) \leftarrow \frac{N(s_t, a_t)Q(s_t, a_t) + G_t}{N(s_t, a_t) + 1}$, $N(s_t, a_t) \leftarrow N(s_t, a_t) + 1$.
133 The *simulation budget* is the total number of iterations, which is the number of times the search tree
134 is expanded, and therefore the size of the tree.
135136 4.2 PREDICTION FUNCTION
137138 The prediction function of the agent takes an environment state as input and outputs a probability
139 distribution over actions and value estimate. Following Silver et al. (2018), we use a single neural
140 network that outputs both of these. Our experimental settings have states that are naturally modeled
141 as *sets* of objects (such as sets of cities, facilities, targets, boxes, etc.), where each object can be
142 described by a vector (e.g., the coordinates of a city and whether it has been visited or not). Therefore,
143 we seek a neural network architecture that can process a *set* of vectors, rather than just a single vector.
144 Early works on neural networks for processing set inputs include McGregor (2007; 2008).
145146 In our experiments, we use *DeepSets* (Zaheer et al., 2017), a neural network architecture that
147 can process sets of inputs in a way that is equivariant or invariant (depending on the desired type
148 of output) with respect to the inputs. It is known to be a universal approximator for continuous
149 set functions, provided that the model’s latent space is sufficiently high-dimensional (Wagstaff
150 et al., 2022). DeepSets may be viewed as the most efficient incarnation of the Janossy pooling
151 paradigm (Murphy et al., 2018), and can be generalized by Transformers (Vaswani et al., 2017; Kim
152 et al., 2021). A permutation-equivariant layer of the DeepSets architecture has the form (Zaheer
153 et al., 2017, Supplement p. 19) $\mathbf{Y} = \sigma(\mathbf{X} \cdot \mathbf{A} + \mathbf{1} \otimes \mathbf{b} + \mathbf{1} \otimes ((\mathbf{1} \cdot \mathbf{X}) \cdot \mathbf{C}))$ where $\mathbf{X} \in \mathbb{R}^{n \times d}$,
154 $\mathbf{Y} \in \mathbb{R}^{n \times k}$, $\mathbf{A}, \mathbf{C} \in \mathbb{R}^{n \times k}$, $\mathbf{b} \in \mathbb{R}^k$, and $\mathbf{1}$ is the all-ones vector of appropriate dimensionality,
155 and σ is a nonlinear activation function, such as ReLU. Here, n is the size of the set (i.e., number
156 of inputs/outputs), d is the dimension of each input, and k is the dimension of each output. A
157 permutation-invariant layer is simply a permutation-equivariant layer followed by global average
158 pooling (yielding an output that is a vector rather than a matrix) followed by a nonlinearity.
159160 In problems where the action space matches the set of inputs (such as cities in the TSP problem, or
161 points in the vertex k -center and maximum diversity problems), the predicted action logits are read
162 out via a dense layer following the permutation-equivariant layer, before global pooling. In problems
163 where the action space is a fixed set of actions (such as Sokoban and the navigation problems), the
164 predicted action logits are read out via a dense layer following the permutation-invariant layer. In both
165 cases, the predicted value is read out via a dense layer from the output of the permutation-invariant
166 layer.
167

162 For clarity, we emphasize that we use *the exact same architecture* for both AlphaZero and AlphaZe-
 163 roES in each problem. This is an apples-to-apples comparison. The only thing that changes is the
 164 optimization objective. AlphaZero itself is largely agnostic to the particular neural architecture avail-
 165 able to the agent. It has been used in conjunction with simple feedforward networks, convolutional
 166 networks, attention-based networks (which encode permutation invariance), and so on.
 167
 168

169 4.3 TRAINING PROCEDURE

171 We are now ready to present the essential difference between AlphaZero and our AlphaZeroES. The
 172 difference lies in the training objective, which in turn entails a difference in the training procedure.
 173 AlphaZero minimizes a *planning loss*, which is the sum of a value loss $\sum_t (R_t - v_t)^2$ and a *policy*
 174 $\sum_t H(w_t, p_t)$. Here, $(v_t, p_t) = f_\theta(s_t)$ is the predicted state value and action probabilities for
 175 s_t , respectively. $(R_t - v_t)^2$ is the squared difference between v_t and the actual episode return R_t .
 176 $H(w_t, p_t)$ is the cross entropy between the action weights w_t returned by the MCTS algorithm for s_t
 177 and p_t . Our approach keeps *exactly the same* architecture, hyperparameters, and MCTS algorithm as
 178 AlphaZero, but changes the optimization objective. Specifically, instead of minimizing the planning
 179 loss, we *directly maximize the episode score*. The parameters that are optimized are exactly those
 180 of AlphaZero, namely, the neural network parameters of the prediction function. Only the training
 181 objective is different.

182 One way to directly optimize the episode score is to use policy gradient methods, which yield an
 183 estimator of the gradient of the expected return with respect to the agent’s parameters. There is a vast
 184 literature on policy gradient methods, which include REINFORCE (Williams, 1992) and actor-critic
 185 methods (Konda and Tsitsiklis, 1999; Grondman et al., 2012). However, there is a problem. Most
 186 of these methods assume that the policy is *differentiable*—more precisely, that its output action
 187 distribution is differentiable with respect to the parameters of the policy. However, our planning
 188 policy uses MCTS as a subroutine, and standard MCTS is not differentiable. Because our policy
 189 contains a non-differentiable submodule, we need to find an alternative way to optimize the policy’s
 190 parameters. Furthermore, Metz et al. (2021) show that differentiation can fail to be useful when trying
 191 to optimize certain functions—specifically, when working with an iterative differentiable system with
 192 chaotic dynamics. Fortunately, we can turn to black-box (i.e., zeroth-order) optimization. Black-box
 193 optimization uses only function evaluations to optimize a function with respect to a set of inputs.
 194 In particular, it does not require gradients. In our case, the black-box function maps our policy’s
 195 parameters to a sampled episode score.

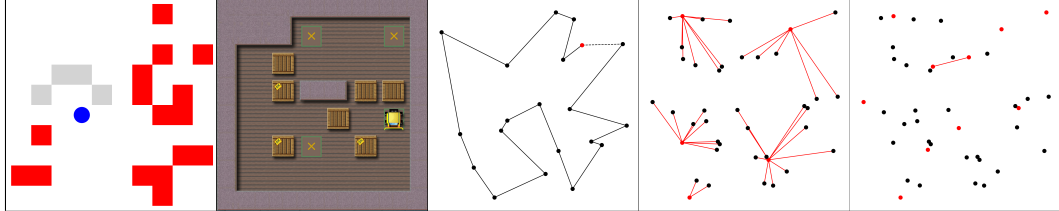
196 There is a class of black-box optimization algorithms called *evolution strategies (ES)* (Rechenberg
 197 and Eigen, 1973; Schwefel, 1977; Rechenberg, 1978) that maintain and evolve a population of
 198 parameter vectors. *Natural evolution strategies (NES)* (Wierstra et al., 2014; Yi et al., 2009) represent
 199 the population as a distribution over parameters and maximize its average objective value using the
 200 score function estimator. For many parameter distributions, such as Gaussian smoothing, this is
 201 equivalent to evaluating the function at randomly-sampled points and estimating the gradient as a
 202 sum of estimates of directional derivatives along random directions (Duchi et al., 2015; Nesterov
 203 and Spokoiny, 2017; Shamir, 2017; Berahas et al., 2022). ES can be used to learn non-differentiable
 204 parameters of large supervised models, such as sparsity masks for weights (Lenc et al., 2019).

205 We use OpenAI-ES (Salimans et al., 2017), an NES algorithm that has been shown to be effective
 206 for reinforcement learning (Salimans et al., 2017), including training large language models (Qiu
 207 et al., 2025). It is based on the identity $\nabla_x E_{z \sim \mathcal{D}} f(x + \sigma z) = \frac{1}{\sigma} E_{z \sim \mathcal{D}} f(x + \sigma z)z$, where \mathcal{D} is the
 208 standard multivariate normal distribution. This algorithm is shown in Algorithm 1. Like Salimans
 209 et al. (2017), we use antithetic sampling (Geweke, 1988), also called mirrored sampling (Brockhoff
 210 et al., 2010), to reduce variance. It samples antithetic pairs of perturbations $(z_i, -z_i)$.

211 This algorithm is massively parallelizable, since each δ_i can be evaluated on a separate worker.
 212 Furthermore, communication between workers is minimal. All workers are initialized with the same
 213 random seed. Worker i evaluates δ_i , sends it to the remaining workers, and receives the other workers’
 214 values (this is called an all-gather operation in distributed computing). Thus the workers compute
 215 the same g and stay synchronized. Again, each worker computes the δ_i corresponding to *its own*
 index i and receives the others from the other workers, but generates the all workers’ perturbation
 vectors $\{z_j\}_{j \in \mathcal{I}}$ itself, which is more efficient than communicating them. The shared random seed

216 **Algorithm 1** Evolution strategies (with a vanilla SGD optimizer).

217
218 **Input:** Initial parameters $\mathbf{x} \in \mathbb{R}^d$, noise scale $\sigma \in \mathbb{R}$, learning rate $\alpha \in \mathbb{R}$, set of workers \mathcal{I} .
219 **for** $t = 0, 1, 2, \dots$ **do**
220 Sample perturbations $\mathbf{z}_1, \dots, \mathbf{z}_n \sim \mathcal{N}(\mathbf{0}_d, I_d)$
221 For each $i \in \mathcal{I}$, let worker i compute $\delta_i \leftarrow f(\mathbf{x} + \sigma \mathbf{z}_i)$
222 Compute pseudogradient $\mathbf{g} \leftarrow \frac{1}{\sigma |\mathcal{I}|} \sum_{i \in \mathcal{I}} \delta_i \mathbf{z}_i$
223 Update parameters $\mathbf{x} \leftarrow \mathbf{x} + \alpha \mathbf{g}$

224
232 Figure 1: Example states for each environment: Navigation, Sokoban, TSP, VKCP, and MDP.
233
234
235 ensures that workers can compute identical perturbation vectors without communication. The only
236 worker-dependent computation is δ_i .
237

238 Notably, AlphaZeroES needs only the parameter perturbation vector \mathbf{z} and the final episode score
239 to update the parameters. In contrast, AlphaZero needs to compute gradients of the parameters via
240 backpropagation (reverse-mode automatic differentiation) through the neural network and over the
241 timesteps of the episode. In our experiments, AlphaZero and AlphaZeroES took about the same
242 amount of time per iteration.
243
244

5 EXPERIMENTS

245
246 In this section, we describe our experiments. We use 10 trials per experiment, 1000 episodes per
247 batch (for both training and evaluation at the end of each epoch), 1000 training batches per epoch,
248 4 hours of training time per trial, the AdaBelief (Zhuang et al., 2020) optimizer¹, a perturbation
249 scale of 0.1 for OpenAI-ES, an MCTS simulation budget of 8,² hidden layer sizes of 16 for the
250 DeepSets network, 1 equivariant plus 1 invariant hidden layer for the DeepSets network, and the
251 ReLU activation function. We used an NVIDIA A100 SXM4 40GB GPU. Each trial uses 1 such GPU
252 all to itself. This keeps the comparison between AlphaZero and AlphaZeroES as precise as possible.
253 For our code, we use Python 3.12.2, JAX 0.4.28 (Bradbury et al., 2018), Flax 0.8.3 (Heek et al.,
254 2024), Optax 0.2.2 (DeepMind et al., 2020), Mctx 0.0.5 (DeepMind et al., 2020), and Matplotlib
255 3.8.4 (Hunter, 2007). In our plots, we show the episode scores attained by AlphaZero (labeled es=0
256 in the plot legend) vs. AlphaZeroES (labeled es=1 in the plot legend). At any point along the X axis,
257 AlphaZero and AlphaZeroES have undergone the same number of episodes of learning. To perform
258 a fair comparison, since AlphaZero and AlphaZeroES optimize different objectives, we test both
259 across a wide range of learning rates (labeled 1r in the plot legend). In addition, we show value
260 and policy losses over the course of training. Though AlphaZeroES does not optimize these losses
261 directly, we wish to observe what happens to them as a side-effect of maximizing the episode score.
262 Solid lines show the mean across trials, and bands show the standard error of the mean. Our goal is
263 not to develop the best special-purpose solver for any one of these domains. Rather, we are interested
264 in a *general*-purpose approach that can tackle *all* of these domains and learn good heuristics on its
265 own. Due to space constraints, we relegate the plots showing value and policy loss to the appendix.

266
267 ¹Both AlphaZero and AlphaZeroES can be combined with any optimizer from the literature. Finding the
268 best optimizer is not the focus of this paper. AdaBelief is a well-known optimizer with many citations. We chose
269 it because it is (a) relatively well-known and (b) outperforms SGD and Adam.

270 ²Gumbel Muzero, the AlphaZero variant we use, can learn reliably with as few as 2 simulations, and was
271 evaluated in its paper with 2, 4, and 16 simulations (Danihelka et al., 2022, p. 8).

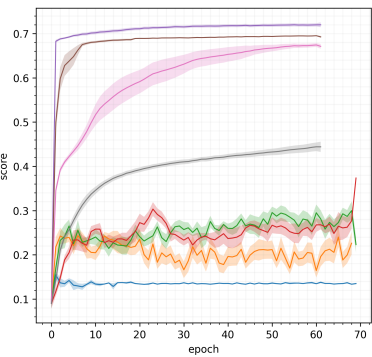


Figure 2: Navigation score.

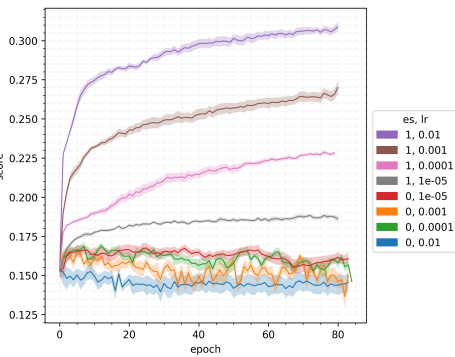


Figure 3: Sokoban score.

5.1 NAVIGATION

In this environment, an agent navigates a gridworld to reach as many targets as possible within a given time limit. At the beginning of each episode, targets are placed uniformly at random in a 10×10 grid, as is the agent. On each timestep, the agent can move up, down, left, or right by one tile. The agent reaches a target when it moves into the same tile. The agent receives a reward of $+0.05$ when it reaches a target. Thus the agent is incentivized to reach as many targets as possible within the time limit. For our experiments, we use 20 targets and a time limit of 50 steps. The prediction network observes a set of vectors, one for each target, where each vector contains the coordinates of the target, a boolean 0-1 flag indicating whether it has already been reached, and the number of episode timesteps remaining. This environment has been used before as a benchmark by Oh et al. (2017, §4.2). It resembles a traveling salesman-like problem in which several “micro” actions are required to perform the “macro” actions of moving from one city to another. (Also, the agent can visit cities multiple times and does not need to return to its starting city.) This models situations where several fine-grained actions are required to perform relevant tasks, such as moving a unit in a real-time strategy game a large distance across the map.

An example state is shown in Figure 1. The blue circle is the agent. Red squares are unreached targets. Gray squares are reached targets. Experimental results are shown in Figure 2 and 7. AlphaZeroES dramatically outperforms AlphaZero. Unlike AlphaZero, it does not seem to minimize the value and policy losses by a noticeable amount. In fact, for AlphaZeroES, the value and policy losses seem to *increase* over time as training proceeds (and the mean episode score increases). This will be a recurring pattern across environments, as we will observe with the other benchmarks. This phenomenon suggests that maximizing “self-consistency” via planning loss minimization, as standard AlphaZero does, is not necessarily aligned as an objective with performing better in the environment, as measured by mean episode score.

5.2 SOKOBAN

Sokoban is a puzzle in which an agent pushes boxes around a warehouse to get them to storage locations. It is played on a grid of tiles. Each tile may be a floor or a wall, and may contain a box or the agent. Some floor tiles are marked as storage locations. The agent can move horizontally or vertically onto empty tiles. The agent can also move a box by walking up to it and push it to the tile beyond, if the latter is empty. Boxes cannot be pulled, and they cannot be pushed to squares with walls or other boxes. The number of boxes equals the number of storage locations. The puzzle is solved when all boxes are placed at storage locations. Planning ahead is crucial, since an agent can easily get stuck if it makes the wrong move. Sokoban has been studied in the field of computational complexity and shown to be PSPACE-complete (Culberson, 1997). It has received significant interest in artificial intelligence research because of its relevance to automated planning (e.g., for autonomous robots), and is used as a benchmark. Sokoban’s large branching factor and search tree depth contribute to its difficulty. Skilled human players rely mostly on heuristics and can quickly discard several futile or redundant lines of play by recognizing patterns and subgoals, narrowing down the search significantly. Various automatic solvers have been developed in the literature (Junghanns and Schaeffer, 1997;

324 2001; Froleyks and Balyo, 2016; Shoham and Schaeffer, 2020), many of which rely on heuristics, but
 325 more complex Sokoban levels remain a challenge.

326 Our environment is as follows. We use the unfiltered Boxoban training set (Guez et al., 2019), which
 327 contains 900,000 levels of size 10×10 each. At the beginning of each episode, we sample a level
 328 from this dataset. As a form of data augmentation, we sample one of the eight symmetries of the
 329 square (a horizontal flip, vertical flip, and/or 90-degree rotation) and apply it to the level. In each
 330 timestep, the agent has four actions available to it, for motion in each of the four cardinal directions.
 331 The level ends after a specified number of timesteps. (We use 50 timesteps.) The return at the end
 332 of an episode is the number of goals that are covered with boxes. Thus the agent is incentivized
 333 to cover all of the goals. The prediction network observes a set of vectors, one for each tile in the
 334 level, where each vector contains the 2 coordinates of the tile, 4 boolean flags indicating whether
 335 the tile contains a wall, goal, box, and/or agent, and the number of episode timesteps remaining. An
 336 example state is shown in Figure 1. This was rendered by JSoko (Meger, 2023), an open-source
 337 Sokoban implementation. The yellow vehicle is the agent, who must push the brown boxes into the
 338 goal squares marked with Xs. (Boxes tagged “OK” are on top of goal squares.) Experimental results
 339 are shown in Figure 3 and 8. AlphaZeroES dramatically outperforms AlphaZero. Unlike AlphaZero,
 340 it does not seem to minimize the value and policy losses by a noticeable amount.

341 5.3 TSP

342 The *traveling salesman problem (TSP)* is a classic combinatorial optimization problem. Given a
 343 set of cities and their pairwise distances, the goal is to find a shortest route that visits each city
 344 once and returns to the starting city. This problem has important applications in operations research,
 345 including logistics, computer wiring, vehicle routing, and various other planning problems (Matai
 346 et al., 2010). TSP is known to be NP-hard (Karp, 1972), even in the Euclidean setting (Papadimitriou,
 347 1977). Various approximation algorithms and heuristics (Nilsson, 2003) have been developed for
 348 it. Our environment is as follows. We seek to learn to solve TSP in general, not just one particular
 349 instance of it. Thus, on every episode, a new problem instance is generated by sampling a matrix
 350 $\mathbf{X} \sim \text{Uniform}([0, 1]^{n \times 2})$, representing a sequence of $n \in \mathbb{N}$ cities. In our experiments, we use
 351 $n = 20$. At timestep $t \in [n]$, the agent chooses a city $a_t \in [n]$ that has not been visited yet. At
 352 the end of the episode, the length of the tour through this sequence of cities (including the segment
 353 from the final city to the initial one) is computed, and treated as the *negative* score. Thus the
 354 agent is incentivized to find the shortest tour through all the cities. Formally, the final score is
 355 $-\sum_{t \leq n} d(\mathbf{X}_{a_t}, \mathbf{X}_{a_{t+1} \bmod n})$, where d is the Euclidean metric. The prediction network observes a
 356 set of vectors, one for each city, where each vector contains the coordinates of the city and 3 boolean
 357 0-1 flags indicating whether it has already been visited, whether it is the initial city, and whether it is
 358 the current city.

359 An example state is shown in Figure 1. Dots are cities. The red dot is the initial city. The lines
 360 connecting the dots constitute the constructed path. The dotted line is the last leg from the final city
 361 back to the initial city. Experimental results are shown in Figure 4 and 9. AlphaZeroES dramatically
 362 outperforms AlphaZero. Interestingly, as a side effect, it minimizes the policy loss about as much as
 363 AlphaZero does. It also minimizes the value loss (except at the highest learning rate), though to a
 364 lesser extent than AlphaZero.

365 5.4 VKCP

366 The *vertex k -center problem (VKCP)* is a classic combinatorial optimization problem that has
 367 applications in facility location and clustering. The problem is as follows. Given n points in \mathbb{R}^d ,
 368 select a subset \mathcal{S} of k points that minimizes the distance from any point in the original set to its nearest
 369 point in \mathcal{S} . The n points can be interpreted as possible locations in which to build facilities (e.g., fire
 370 stations, police stations, supply depots, etc.), where \mathcal{S} is the set of locations in which such facilities
 371 are built, and the goal is to minimize the maximum distance from any location to its nearest facility.
 372 (There is also a variant of the problem that seeks to minimize the *mean* distance.) This problem was
 373 first proposed by Hakimi (1964). It is NP-hard, and various approximation algorithms have been
 374 proposed for it (Kariv and Hakimi, 1979; Gonzalez, 1985; Dyer and Frieze, 1985; Hochbaum and
 375 Shmoys, 1985; Shmoys, 1994). A survey and evaluation of approximation algorithms can be found
 376 in Garcia-Diaz et al. (2019).

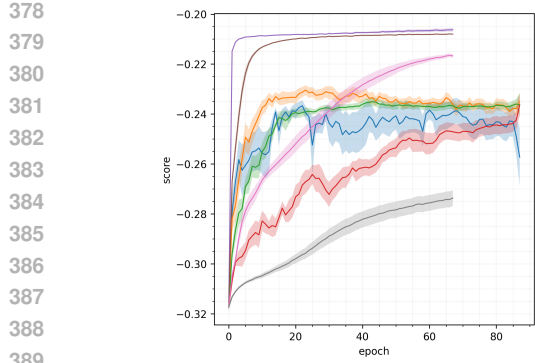


Figure 4: TSP score.

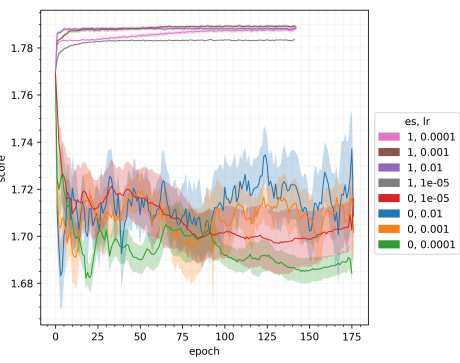


Figure 5: VKCP score.

393 We sample $n = 40$ locations uniformly at random from the unit square and let $k = 20$. At any
394 timestep t , the agent selects a location $a_t \in [n]$ that has not been selected yet to add a facility at
395 that location. The final score is $-\max_{i \in [n]} \min_{j \in \mathcal{S}} d(\mathbf{x}_i, \mathbf{x}_j)$, where $\mathbf{x}_i \in [0, 1]^2$ is the position of
396 point $i \in [n]$ and d is the Euclidean metric. The prediction network observes a set of vectors, one
397 for each point, where each vector contains the coordinates of the point and a single bit indicating
398 whether it is in the subset \mathcal{S} . An example state is shown in Figure 1. Black dots are locations, red
399 dots are facilities placed so far, and red lines connect locations to their nearest facility. Experimental
400 results are shown in Figure 5 and 10. AlphaZeroES dramatically outperforms AlphaZero. In this
401 environment, AlphaZeroES hardly minimizes the value and policy losses as a side effect.

5.5 MDP

405 In the *maximum diversity problem (MDP)*, we
406 are given n points in \mathbb{R}^d , and we are asked to
407 select a subset \mathcal{S} of k points that maximizes
408 the minimum distance between distinct points.
409 (There is also a variant of the problem that seeks
410 to maximize the *mean* distance between dis-
411 tinct points.) This problem is strongly NP-hard,
412 as can be shown via reduction from the clique
413 problem (Kuo et al., 1993; Ghosh, 1996). Vari-
414 ous heuristics have been proposed for it (Glover
415 et al., 1998; Katayama and Narihisa, 2005; Silva
416 et al., 2007; Duarte and Martí, 2007; Martí et al.,
417 2010; Lozano et al., 2011; Wu and Hao, 2013;
418 Martí et al., 2013). This problem has applica-
419 tions in ecology, medical treatment, genetic
420 engineering, capital investment, pollution control,
421 system reliability, telecommunication services,
422 molecular structure design, transportation sys-
423 tem control, emergency service centers, and energy options, as cataloged by Glover et al. (1998,
424 Table 1).

425 For our experiments, we sample $n = 40$ locations uniformly at random from the unit square and
426 let $k = 20$. At any timestep t , the agent can select a point $a_t \in [n]$ that has not been selected yet
427 to add to the set \mathcal{S} . The final score is $\min_{i, j \in \mathcal{S}, i \neq j} d(\mathbf{x}_i, \mathbf{x}_j)$, where $\mathbf{x}_i \in [0, 1]^2$ is the position of
428 point i and d is the Euclidean metric. The prediction network observes a set of vectors, one for each
429 point, where each vector contains the coordinates of the point and a bit flag indicating whether it
430 has been included in the set. An example state is shown in Figure 1. Black dots are points, red dots
431 are points selected so far, and the red line connects the closest pair of points in the set selected so
432 far. Experimental results are shown in Figure 6 and 11. AlphaZeroES dramatically outperforms
433 AlphaZero. As a side effect, it minimizes the policy loss about as much as AlphaZero does. However,
434 unlike AlphaZero, it does not seem to minimize the value loss.

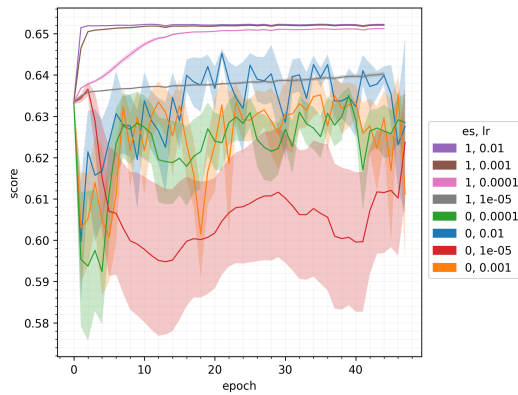


Figure 6: MDP score.

432

6 DISCUSSION

433
 434 **Why does our method work?** Our method did not drive value and policy losses down to zero, as
 435 standard AlphaZero does, suggesting that maximizing “self-consistency” is not necessarily required
 436 to perform better in the environment in terms of score. One reason might be that optimal or strong
 437 performance does not actually require *internal consistency* (of value and action predictions), and
 438 achieving *good performance* might be easier than achieving internal consistency.

439 There are situations where learning a good policy is easy, but learning a good function is hard.
 440 Consider an environment where there is a simple optimal policy, but the value function under that
 441 policy is complicated—that is, for any given state, it is easy to determine what the “right” action
 442 to take is, but difficult to predict the final return. AlphaZero’s performance intrinsically depends
 443 on the accuracy of its learned value function, since that value function is used as an oracle inside
 444 the MCTS algorithm in a way that ultimately determines what action to take. If this value function
 445 is difficult to learn, AlphaZero might struggle. In fact, even being *semi-accurate* with respect to
 446 values does not, in and of itself, guarantee good action selection. The value estimates also need to be
 447 *order-accurate*—that is, accurate with respect to their relative rankings or differences—since this
 448 ultimately determines which actions MCTS chooses.

449 On the other hand, AlphaZeroES has the flexibility to simply optimize a policy directly, even if it has
 450 not learned an accurate value function for it. The value function being accurate might be helpful, but
 451 is not necessary. In summary, direct policy methods sometimes succeed where value-based methods
 452 fail. This can happen when a good policy is more easily representable (and learnable) than a good
 453 value function. In those cases, direct policy improvement can easily yield a good policy. Conversely,
 454 relying on a poorly-approximated critic can actually *hamper* performance. To illustrate this point,
 455 in the appendix, we give concrete examples of *simple* environments where AlphaZero fails while
 456 AlphaZeroES succeeds. In the appendix, we also include an ablation study that investigates whether
 457 the improvement of AlphaZeroES over AlphaZero comes mostly from an improved value output or
 458 an improved policy output. Interestingly, the answer is environment-dependent.

459

7 CONCLUSIONS AND FUTURE RESEARCH

460 In this paper, we set out to study whether AlphaZero and its newest variants can be improved by
 461 maximizing the episode score directly instead of minimizing the standard planning loss. Since MCTS
 462 is not differentiable, we maximize the episode score by using evolution strategies. We conducted
 463 experiments across multiple domains, including standard combinatorial optimization problems and
 464 motion planning problems from the literature. In each setting, our approach yielded a dramatic
 465 improvement in performance over planning loss minimization.

466 Our work opens up new possibilities for tackling environments where planning is important. It does
 467 this by allowing agents to learn to leverage internal nondifferentiable planning algorithms, such as
 468 MCTS, *in a purely blackbox way* that does not depend on the internal details of those algorithms.
 469 Instead of training the agent’s parameters to minimize some indirect proxy objective, such as a
 470 planning loss, we can now maximize the desired objective *directly*.

471 **Limitations** The original AlphaZero and Gumbel MuZero MCTS algorithms are designed for
 472 fully-observable deterministic environments. Thus, so is our method. An extension to stochastic
 473 environments exists in the form of Stochastic MuZero (Antonoglou et al., 2022). By replacing the
 474 MCTS algorithm with that of Stochastic MuZero, it might be possible to extend our method to
 475 stochastic environments. Another potential direction for future research might be to extend our work
 476 to adversarial or multiagent settings. Doing so would require introducing concepts from game theory
 477 and making modifications to our method. For example, our method uses ES to maximize the episode
 478 score. However, solving a two-player zero-sum game is not a pure *maximization* problem, but rather
 479 a *min-max* (saddle-point) problem. Solving such a problem requires more sophisticated gradient
 480 dynamics. It might be possible to use a modified version of ES to seek equilibria of the players’
 481 individual episode scores with respect to their parameters. Related works for this include Bichler
 482 et al. (2021), Martin and Sandholm (2023), and Martin and Sandholm (2025). This is outside the
 483 scope of this paper, but potentially interesting for future research.

486 REFERENCES
487

488 Allen Newell and George Ernst. The search for generality. In *Proc. IFIP Congress*, 1965.

489 Peter Hart, Nils Nilsson, and Bertram Raphael. A formal basis for the heuristic determination of
490 minimum cost paths. *IEEE transactions on Systems Science and Cybernetics*, 1968.

491

492 Nils Nilsson. Problem-solving methods in artificial intelligence. *Artificial Intelligence*, 1971.

493

494 Peter E. Hart, Nils J. Nilsson, and Bertram Raphael. Correction to “a formal basis for the heuristic
495 determination of minimum cost paths”. *ACM SIGART Bulletin*, 1972.

496

497 Marc Lanctot, Vinicius Zambaldi, Audrunas Gruslys, Angeliki Lazaridou, Karl Tuyls, Julien Pérolat,
498 David Silver, and Thore Graepel. A unified game-theoretic approach to multiagent reinforcement
499 learning. *Conference on Neural Information Processing Systems (NeurIPS)*, 2017.

500

501 Noam Brown et al. Depth-limited solving for imperfect-information games. In *NeurIPS*, 2018.

502

503 Rémi Coulom. Efficient selectivity and backup operators in Monte-Carlo tree search. In *Computers
and Games*, 2007.

504

505 David Silver, Aja Huang, Chris J. Maddison, Arthur Guez, Laurent Sifre, George van den Driessche,
506 Julian Schrittwieser, Ioannis Antonoglou, Veda Panneershelvam, Marc Lanctot, Sander Dieleman,
507 Dominik Grewe, John Nham, Nal Kalchbrenner, Ilya Sutskever, Timothy Lillicrap, Madeleine
508 Leach, Koray Kavukcuoglu, Thore Graepel, and Demis Hassabis. Mastering the game of Go with
deep neural networks and tree search. *Nature*, 2016.

509

510 David Silver, Julian Schrittwieser, Karen Simonyan, Ioannis Antonoglou, Aja Huang, Arthur Guez,
511 Thomas Hubert, Lucas Baker, Matthew Lai, Adrian Bolton, Yutian Chen, Timothy Lillicrap, Fan
512 Hui, Laurent Sifre, George van den Driessche, Thore Graepel, and Demis Hassabis. Mastering the
513 game of Go without human knowledge. *Nature*, 2017a.

514

515 David Silver, Thomas Hubert, Julian Schrittwieser, Ioannis Antonoglou, Matthew Lai, Arthur
516 Guez, Marc Lanctot, Laurent Sifre, Dharshan Kumaran, Thore Graepel, Timothy Lillicrap, Karen
517 Simonyan, and Demis Hassabis. A general reinforcement learning algorithm that masters chess,
shogi, and Go through self-play. *Science*, 2018.

518

519 Julian Schrittwieser, Ioannis Antonoglou, Thomas Hubert, Karen Simonyan, Laurent Sifre, Simon
520 Schmitt, Arthur Guez, Edward Lockhart, Demis Hassabis, Thore Graepel, Timothy Lillicrap, and
521 David Silver. Mastering atari, Go, chess and shogi by planning with a learned model. *Nature*,
2020.

522

523 Ivo Danihelka, Arthur Guez, Julian Schrittwieser, and David Silver. Policy improvement by planning
524 with Gumbel. In *International Conference on Learning Representations (ICLR)*, 2022.

525

526 Maciej Świechowski, Konrad Godlewski, Bartosz Sawicki, and Jacek Mańdziuk. Monte Carlo tree
527 search: a review of recent modifications and applications. *Artificial Intelligence Review*, 2023.

528

529 Mauro Vallati, Lukas Chrpa, Marek Grześ, Thomas Leo McCluskey, Mark Roberts, and Scott Sanner.
The 2014 international planning competition: Progress and trends. *AI Magazine*, 2015.

530

531 Horacio Yanasse and Edson Senne. The minimization of open stacks problem: A review of some
532 properties and their use in pre-processing operations. *European Journal of Operational Research
(EJOR)*, 2010.

533

534 Jan Kuipers, Aske Plaat, Jos A. M. Vermaasen, and H. Jaap van den Herik. Improving multivariate
535 Horner schemes with Monte Carlo tree search. *Computer Physics Communications*, 2013.

536

537 Jie Jia, Jian Chen, and Xingwei Wang. Ultra-high reliable optimization based on Monte Carlo tree
538 search over nakagami-m fading. *Applied Soft Computing*, 2020.

539

Feng Shi, Ranjith K. Soman, Ji Han, and Jennifer K. Whyte. Addressing adjacency constraints in
rectangular floor plans using Monte-Carlo tree search. *Automation in Construction*, 2020.

540 Duncan McElfresh, Michael Curry, Tuomas Sandholm, and John Dickerson. Improving policy-
 541 constrained kidney exchange via pre-screening. *Conference on Neural Information Processing*
 542 *Systems (NeurIPS)*, 2020.

543 Carlos Martin, Craig Boutilier, Ofer Meshi, and Tuomas Sandholm. Model-free preference elicitation.
 544 In *Proceedings of the International Joint Conference on Artificial Intelligence (IJCAI)*, 2024.

545 Kenshin Abe, Zijian Xu, Issei Sato, and Masashi Sugiyama. Solving NP-hard problems on graphs
 546 with extended AlphaGo Zero. *arXiv:1905.11623*, 2019.

547 Alhussein Fawzi, Matej Balog, Aja Huang, Thomas Hubert, Bernardino Romera-Paredes, Moham-
 548 madamin Barekatain, Alexander Novikov, Francisco J. R. Ruiz, Julian Schrittweis, Grzegorz
 549 Swirszcz, David Silver, Demis Hassabis, and Pushmeet Kohli. Discovering faster matrix multipli-
 550 cation algorithms with reinforcement learning. *Nature*, 2022.

551 Ruiyang Xu and Karl Lieberherr. Learning self-game-play agents for combinatorial optimization
 552 problems. *arXiv:1903.03674*, 2019.

553 DeepMind, Igor Babuschkin, Kate Baumli, Alison Bell, Surya Bhupatiraju, Jake Bruce, Peter
 554 Buchlovsy, David Budden, Trevor Cai, Aidan Clark, Ivo Danihelka, Antoine Dedieu, Clau-
 555 dio Fantacci, Jonathan Godwin, Chris Jones, Ross Hemsley, Tom Hennigan, Matteo Hessel,
 556 Shaobo Hou, Steven Kapturowski, Thomas Keck, Iurii Kemaev, Michael King, Markus Kunesch,
 557 Lena Martens, Hamza Merzic, Vladimir Mikulik, Tamara Norman, George Papamakarios, John
 558 Quan, Roman Ring, Francisco Ruiz, Alvaro Sanchez, Laurent Sartran, Rosalia Schneider,
 559 Eren Sezener, Stephen Spencer, Srivatsan Srinivasan, Miloš Stanojević, Wojciech Stokowiec,
 560 Luyu Wang, Guangyao Zhou, and Fabio Viola. The DeepMind JAX Ecosystem, 2020. URL
 561 <http://github.com/google-deepmind>.

562 Simon McGregor. Neural network processing for multiset data. In *International Conference on*
 563 *Artificial Neural Networks*, 2007.

564 Simon McGregor. Further results in multiset processing with neural networks. *Neural networks*,
 565 2008.

566 Manzil Zaheer, Satwik Kottur, Siamak Ravanbakhsh, Barnabas Poczos, Russ R Salakhutdinov, and
 567 Alexander J. Smola. Deep Sets. *Conference on Neural Information Processing Systems (NeurIPS)*,
 568 2017.

569 Edward Wagstaff, Fabian B. Fuchs, Martin Engelcke, Michael A. Osborne, and Ingmar Posner.
 570 Universal approximation of functions on sets. *Journal of Machine Learning Research*, 2022.

571 Ryan L. Murphy, Balasubramanian Srinivasan, Vinayak Rao, and Bruno Ribeiro. Janossy pooling:
 572 Learning deep permutation-invariant functions for variable-size inputs. *arXiv:1811.01900*, 2018.

573 Ashish Vaswani, Noam Shazeer, Niki Parmar, Jakob Uszkoreit, Llion Jones, Aidan N. Gomez,
 574 Łukasz Kaiser, and Illia Polosukhin. Attention is all you need. *Conference on Neural Information*
 575 *Processing Systems (NeurIPS)*, 2017.

576 Jinwoo Kim, Saeyoon Oh, and Seunghoon Hong. Transformers generalize deepsets and can be
 577 extended to graphs & hypergraphs. *Conference on Neural Information Processing Systems*
 578 (*NeurIPS*), 2021.

579 Ronald Williams. Simple statistical gradient-following algorithms for connectionist reinforcement
 580 learning. *Machine Learning*, 1992.

581 Vijay Konda and John Tsitsiklis. Actor-critic algorithms. In *Conference on Neural Information*
 582 *Processing Systems (NeurIPS)*, 1999.

583 Ivo Grondman, Lucian Busoniu, Gabriel A. D. Lopes, and Robert Babuska. A survey of actor-critic
 584 reinforcement learning: standard and natural policy gradients. *IEEE Transactions on Systems,*
 585 *Man, and Cybernetics, Part C (Applications and Reviews)*, 2012.

586 Luke Metz, C. Daniel Freeman, Samuel S. Schoenholz, and Tal Kachman. Gradients are not all you
 587 need. *arXiv:2111.05803*, 2021.

594 Ingo Rechenberg and Manfred Eigen. *Evolutionsstrategie: Optimierung technischer Systeme nach*
 595 *Prinzipien der biologischen Evolution*. Frommann-Holzboog Stuttgart, 1973.

596

597 Hans-Paul Schwefel. *Numerische Optimierung von Computer-Modellen mittels der Evolutionsstrate-*
 598 *gie*. Birkhäuser Basel, 1977.

599 Ingo Rechenberg. Evolutionsstrategien. In *Simulationsmethoden in der Medizin und Biologie*.
 600 Springer, 1978.

601

602 Daan Wierstra, Tom Schaul, Tobias Glasmachers, Yi Sun, Jan Peters, and Jürgen Schmidhuber.
 603 Natural evolution strategies. *Journal of Machine Learning Research*, 2014.

604 Sun Yi, Daan Wierstra, Tom Schaul, and Jürgen Schmidhuber. Stochastic search using the natural
 605 gradient. In *International Conference on Machine Learning (ICML)*, 2009.

606

607 John C. Duchi, Michael I. Jordan, Martin J. Wainwright, and Andre Wibisono. Optimal rates for
 608 zero-order convex optimization: the power of two function evaluations. *IEEE Transactions on*
 609 *Information Theory*, 2015.

610 Yurii Nesterov and Vladimir Spokoiny. Random gradient-free minimization of convex functions.
 611 *Foundations of Computational Mathematics*, 2017.

612 Ohad Shamir. An optimal algorithm for bandit and zero-order convex optimization with two-point
 613 feedback. *Journal of Machine Learning Research*, 2017.

614

615 Albert S. Berahas, Liyuan Cao, Krzysztof Choromanski, and Katya Scheinberg. A theoretical and
 616 empirical comparison of gradient approximations in derivative-free optimization. *Foundations of*
 617 *Computational Mathematics*, 2022.

618 Karel Lenc, Erich Elsen, Tom Schaul, and Karen Simonyan. Non-differentiable supervised learning
 619 with evolution strategies and hybrid methods. *arXiv:1906.03139*, 2019.

620

621 Tim Salimans, Jonathan Ho, Xi Chen, Szymon Sidor, and Ilya Sutskever. Evolution strategies as a
 622 scalable alternative to reinforcement learning. *arXiv:1703.03864*, 2017.

623

624 Xin Qiu, Yulu Gan, Conor F Hayes, Qiyo Liang, Elliot Meyerson, Babak Hodjat, and Risto
 625 Miikkulainen. Evolution strategies at scale: LLM fine-tuning beyond reinforcement learning.
 626 *arXiv:2509.24372*, 2025.

627

628 John Geweke. Antithetic acceleration of Monte Carlo integration in Bayesian inference. *Journal of*
Econometrics, 1988.

629

630 Dimo Brockhoff, Anne Auger, Nikolaus Hansen, Dirk V. Arnold, and Tim Hohm. Mirrored sampling
 631 and sequential selection for evolution strategies. In *Parallel Problem Solving from Nature, PPSN*
XI, 2010.

632

633 Juntang Zhuang, Tommy Tang, Yifan Ding, Sekhar C Tatikonda, Nicha Dvornek, Xenophon Pa-
 634 pademetris, and James Duncan. AdaBelief optimizer: Adapting stepsizes by the belief in observed
 635 gradients. *Conference on Neural Information Processing Systems (NeurIPS)*, 2020.

636

637 James Bradbury, Roy Frostig, Peter Hawkins, Matthew James Johnson, Chris Leary, Dougal
 638 Maclaurin, George Necula, Adam Paszke, Jake VanderPlas, Skye Wanderman-Milne, and
 639 Qiao Zhang. JAX: composable transformations of Python+NumPy programs, 2018. URL
<http://github.com/jax-ml/jax>.

640

641 Jonathan Heek, Anselm Levskaya, Avital Oliver, Marvin Ritter, Bertrand Rondepierre, Andreas
 642 Steiner, and Marc van Zee. Flax: A neural network library and ecosystem for JAX, 2024. URL
<http://github.com/google/flax>.

643

644 John Hunter. Matplotlib: A 2D graphics environment. *Computing in Science & Engineering*, 2007.

645

646 Junhyuk Oh, Satinder Singh, and Honglak Lee. Value prediction network. In *Conference on Neural*
Information Processing Systems (NeurIPS), 2017.

647

Joseph Culberson. Sokoban is PSPACE-complete. Technical report, University of Alberta, 1997.

648 Andreas Junghanns and Jonathan Schaeffer. Sokoban: A challenging single-agent search problem. In
 649 *IJCAI Workshop on Using Games as an Experimental Testbed for AI Research*, 1997.
 650

651 Andreas Junghanns and Jonathan Schaeffer. Sokoban: Enhancing general single-agent search methods
 652 using domain knowledge. *Artificial Intelligence*, 2001.

653 Nils Froleyks and Tomás Balyo. *Using an algorithm portfolio to solve Sokoban*. PhD thesis,
 654 Karlsruher Institut für Technologie (KIT), 2016.
 655

656 Yaron Shoham and Jonathan Schaeffer. The FESS algorithm: A feature based approach to single-agent
 657 search. In *IEEE Conference on Games (CoG)*, 2020.

658 Arthur Guez, Mehdi Mirza, Karol Gregor, Rishabh Kabra, Sebastien Racaniere, Theophane Weber,
 659 David Raposo, Adam Santoro, Laurent Orseau, Tom Eccles, Greg Wayne, David Silver, and
 660 Timothy Lillicrap. An investigation of model-free planning. In *International Conference on
 661 Machine Learning (ICML)*, pages 2464–2473. Proceedings of Machine Learning Research (PMLR),
 662 2019.

663 Matthias Meger. JSoko – website of the open source Sokoban game JSoko, 2023. URL <https://jsokoapplet.sourceforge.io/>.
 664
 665

666 Rajesh Matai, Surya Singh, and Murari Lal Mittal. Traveling salesman problem: an overview of
 667 applications, formulations, and solution approaches. *Traveling salesman problem, theory and
 668 applications*, 2010.

669 Richard Karp. *Reducibility among combinatorial problems*. Springer, 1972.
 670

671 Christos Papadimitriou. The Euclidean travelling salesman problem is NP-complete. *Theoretical
 672 computer science*, 1977.

673 Christian Nilsson. Heuristics for the traveling salesman problem. *Linkoping University*, 2003.
 674

675 S. Louis Hakimi. Optimum locations of switching centers and the absolute centers and medians of a
 676 graph. *Operations research*, 1964.

677 Oded Kariv and S. Louis Hakimi. An algorithmic approach to network location problems. I: The
 678 p-centers. *SIAM journal on applied mathematics*, 1979.
 679

680 Teofilo Gonzalez. Clustering to minimize the maximum intercluster distance. *Theoretical computer
 681 science*, 1985.

682 Martin Dyer and Alan Frieze. A simple heuristic for the p-centre problem. *Operations Research
 683 Letters*, 1985.
 684

685 Dorit Hochbaum and David Shmoys. A best possible heuristic for the k-center problem. *Mathematics
 686 of operations research*, 1985.

687 D. Shmoys. Computing near-optimal solutions to combinatorial optimization problems. Technical
 688 report, Cornell University Operations Research and Industrial Engineering, 1994.
 689

690 Jesus Garcia-Diaz, Rolando Menchaca-Mendez, Ricardo Menchaca-Mendez, Saúl Pomares Hernán-
 691 dez, Julio César Pérez-Sansalvador, and Noureddine Lakouari. Approximation algorithms for the
 692 vertex k-center problem: Survey and experimental evaluation. *IEEE Access*, 2019.

693 Ching-Chung Kuo, Fred Glover, and Krishna S. Dhir. Analyzing and modeling the maximum diversity
 694 problem by zero-one programming. *Decision Sciences*, 1993.
 695

696 Jay Ghosh. Computational aspects of the maximum diversity problem. *Operations research letters*,
 697 1996.

698 Fred Glover, Ching-Chung Kuo, and Krishna S. Dhir. Heuristic algorithms for the maximum diversity
 699 problem. *Journal of information and Optimization Sciences*, 1998.
 700

701 Kengo Katayama and Hiroyuki Narihisa. An evolutionary approach for the maximum diversity
 702 problem. In *Recent advances in memetic algorithms*. Springer, 2005.

702 Geiza C. Silva, Marcos R. Q. De Andrade, Luiz S. Ochi, Simone L. Martins, and Alexandre Plastino.
 703 New heuristics for the maximum diversity problem. *Journal of Heuristics*, 2007.
 704

705 Abraham Duarte and Rafael Martí. Tabu search and grasp for the maximum diversity problem.
 706 *European Journal of Operational Research (EJOR)*, 2007.

707 Rafael Martí, Micael Gallego, and Abraham Duarte. A branch and bound algorithm for the maximum
 708 diversity problem. *European Journal of Operational Research (EJOR)*, 2010.
 709

710 Manuel Lozano, Daniel Molina, and C. Garcí. Iterated greedy for the maximum diversity problem.
 711 *European Journal of Operational Research (EJOR)*, 2011.

712 Qinghua Wu and Jin-Kao Hao. A hybrid metaheuristic method for the maximum diversity problem.
 713 *European Journal of Operational Research (EJOR)*, 2013.
 714

715 Rafael Martí, Micael Gallego, Abraham Duarte, and Eduardo G. Pardo. Heuristics and metaheuristics
 716 for the maximum diversity problem. *Journal of Heuristics*, 2013.

717 Ioannis Antonoglou, Julian Schrittwieser, Sherjil Ozair, Thomas K. Hubert, and David Silver. Plan-
 718 ning in stochastic environments with a learned model. In *International Conference on Learning
 719 Representations (ICLR)*, 2022.

720 Martin Bichler, Maximilian Fichtl, Stefan Heidekrüger, Nils Kohring, and Paul Sutterer. Learning
 721 equilibria in symmetric auction games using artificial neural networks. *Nature Machine Intelligence*,
 722 2021.

723 Carlos Martin and Tuomas Sandholm. Finding mixed-strategy equilibria of continuous-action games
 724 without gradients using randomized policy networks. In *Proceedings of the International Joint
 725 Conference on Artificial Intelligence (IJCAI)*, 2023.

726 Carlos Martin and Tuomas Sandholm. Joint-perturbation simultaneous pseudo-gradient. In *Proceed-
 727 ings of the International Joint Conference on Artificial Intelligence (IJCAI)*, 2025.

728 Aviv Tamar, YI WU, Garrett Thomas, Sergey Levine, and Pieter Abbeel. Value iteration networks. In
 729 *Conference on Neural Information Processing Systems (NeurIPS)*, 2016.

730 David Silver, Hado van Hasselt, Matteo Hessel, Tom Schaul, Arthur Guez, Tim Harley, Gabriel Dulac-
 731 Arnold, David Reichert, Neil Rabinowitz, Andre Barreto, and Thomas Degrif. The predictron:
 732 end-to-end learning and planning. In *International Conference on Machine Learning (ICML)*,
 2017b.

733 Sébastien Racanière, Theophane Weber, David Reichert, Lars Buesing, Arthur Guez, Danilo
 734 Jimenez Rezende, Adrià Puigdomènech Badia, Oriol Vinyals, Nicolas Heess, Yujia Li, Razvan Pas-
 735 canu, Peter Battaglia, Demis Hassabis, David Silver, and Daan Wierstra. Imagination-augmented
 736 agents for deep reinforcement learning. *Conference on Neural Information Processing Systems
 737 (NeurIPS)*, 2017.

738 Arthur Guez, Theophane Weber, Ioannis Antonoglou, Karen Simonyan, Oriol Vinyals, Daan Wierstra,
 739 Remi Munos, and David Silver. Learning to search with MCTSnets. In *International Conference
 740 on Machine Learning (ICML)*, 2018.

741 Gregory Farquhar, Tim Rocktaeschel, Maximilian Igl, and Shimon Whiteson. TreeQN and ATreeC:
 742 Differentiable tree planning for deep reinforcement learning. In *International Conference on
 743 Learning Representations (ICLR)*, 2018.

744 Volodymyr Mnih, Koray Kavukcuoglu, David Silver, Andrei A. Rusu, Joel Veness, Marc G. Belle-
 745 mare, Alex Graves, Martin Riedmiller, Andreas K. Fidjeland, Georg Ostrovski, Stig Petersen,
 746 Charles Beattie, Amir Sadik, Ioannis Antonoglou, Helen King, Dharshan Kumaran, Daan Wierstra,
 747 Shane Legg, and Demis Hassabis. Human-level control through deep reinforcement learning.
 748 *Nature*, 2015.

749 Xuxi Yang, Werner Duvaud, and Peng Wei. Continuous control for searching and planning with a
 750 learned model. *arXiv:2006.07430*, 2020.

756 Thomas Hubert, Julian Schrittwieser, Ioannis Antonoglou, Mohammadamin Barekatain, Simon
 757 Schmitt, and David Silver. Learning and planning in complex action spaces. In *International*
 758 *Conference on Machine Learning (ICML)*, 2021.

759

760 Alexander Schrijver. *Combinatorial optimization: polyhedra and efficiency*. Springer, 2003.

761 John R. Rice. The algorithm selection problem. In *Advances in computers*. Elsevier, 1976.

762

763 Tuomas Sandholm. Very-large-scale generalized combinatorial multi-attribute auctions. In *The*
 764 *Handbook of Market Design*. Oxford University Press, 2013.

765

766 Elias Khalil, Hanjun Dai, Yuyu Zhang, Bistra Dilkina, and Le Song. Learning combinatorial
 767 optimization algorithms over graphs. *Conference on Neural Information Processing Systems*
 768 (*NeurIPS*), 2017.

769

770 Joshua Bengio, Andrea Lodi, and Antoine Prouvost. Machine learning for combinatorial optimization:
 771 a methodological tour d'horizon. *European Journal of Operational Research (EJOR)*, 2021.

772

773 Eric Larsen, Sébastien Lachapelle, Yoshua Bengio, Emma Frejinger, Simon Lacoste-Julien, and
 774 Andrea Lodi. Predicting solution summaries to integer linear programs under imperfect information
 775 with machine learning. *arXiv:1807.11876*, 2018.

776

777 Nina Mazyavkina, Sergey Sviridov, Sergei Ivanov, and Evgeny Burnaev. Reinforcement learning for
 778 combinatorial optimization: A survey. *Computers & Operations Research*, 2021.

779

780 Ruizhong Qiu, Zhiqing Sun, and Yiming Yang. DIMES: A differentiable meta solver for combinatorial
 781 optimization problems. *Conference on Neural Information Processing Systems (NeurIPS)*, 2022.

782

783 Carlo Aironi, Samuele Cornell, and Stefano Squartini. A graph-based neural approach to linear sum
 784 assignment problems. *International Journal of Neural Systems*, 2024.

785

786 Dobrik Georgiev Georgiev, Danilo Numeroso, Davide Baciucc, and Pietro Liò. Neural algorithmic
 787 reasoning for combinatorial optimisation. In *Learning on Graphs Conference*, 2024.

788

789 Maria-Florina Balcan, Travis Dick, Tuomas Sandholm, and Ellen Vitercik. Learning to branch:
 790 Generalization guarantees and limits of data-independent discretization. *Journal of the ACM*, 2024.
 791 Early version in ICML-18.

792

793 Maria-Florina Balcan, Siddharth Prasad, Tuomas Sandholm, and Ellen Vitercik. Sample complexity
 794 of tree search configuration: Cutting planes and beyond. *Conference on Neural Information
 795 Processing Systems (NeurIPS)*, 2021.

796

797 Maria-Florina Balcan, Siddharth Prasad, Tuomas Sandholm, and Ellen Vitercik. Structural analysis
 798 of branch-and-cut and the learnability of Gomory mixed integer cuts. *Conference on Neural
 799 Information Processing Systems (NeurIPS)*, 2022.

800

801 Guangxiang Zhao, Xu Sun, Jingjing Xu, Zhiyuan Zhang, and Liangchen Luo. Muse: Parallel
 802 multi-scale attention for sequence to sequence learning. *arXiv:1911.09483*, 2019.

803

804 Jimmy Lei Ba, Jamie Ryan Kiros, and Geoffrey E Hinton. Layer normalization. *arXiv:1607.06450*,
 805 2016.

806

807 Guido Van Rossum and Fred L. Drake Jr. *Python reference manual*. Centrum voor Wiskunde en
 808 Informatica Amsterdam, 1995.

809

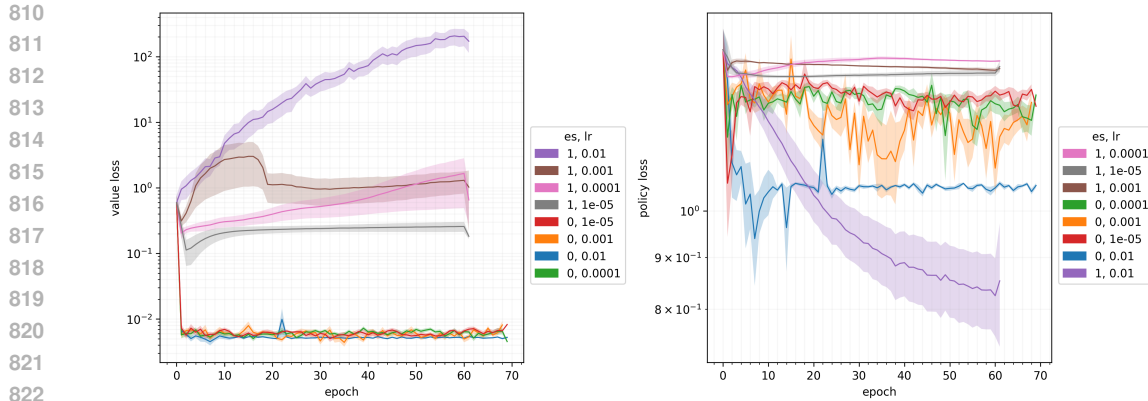


Figure 7: Navigation losses.

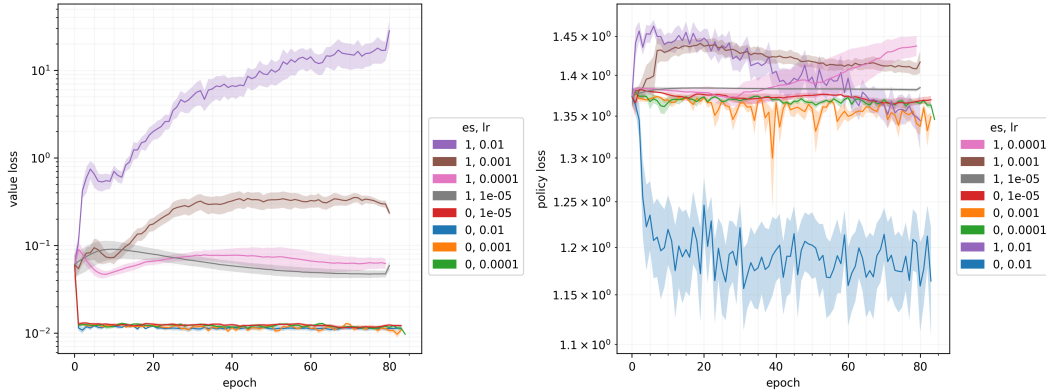


Figure 8: Sokoban losses.

A ADDITIONAL FIGURES

In this section, we include additional figures that did not fit in the body of the paper.

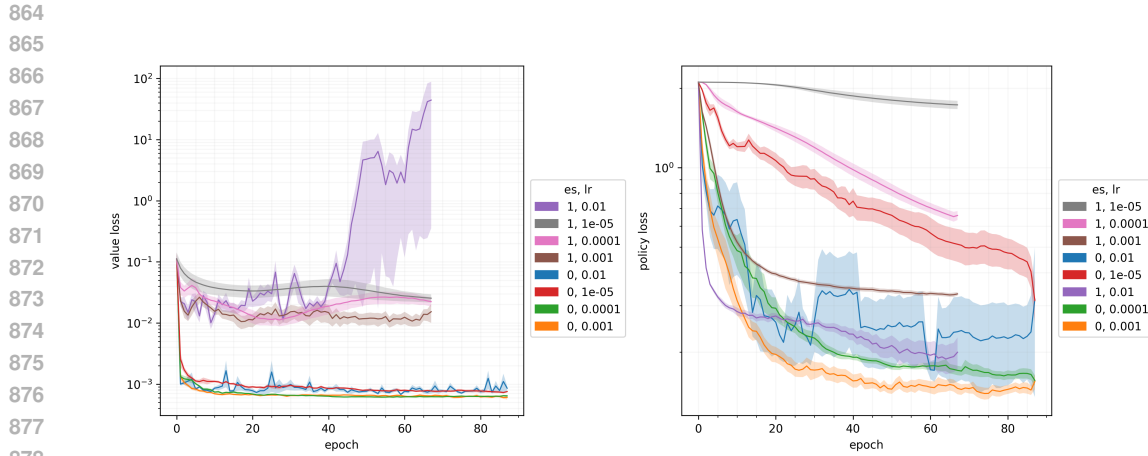


Figure 9: TSP losses.

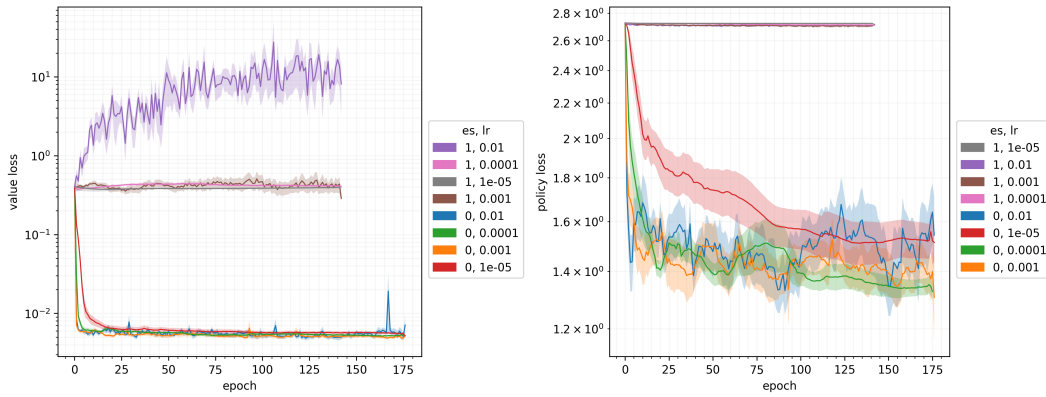


Figure 10: VKCP losses.

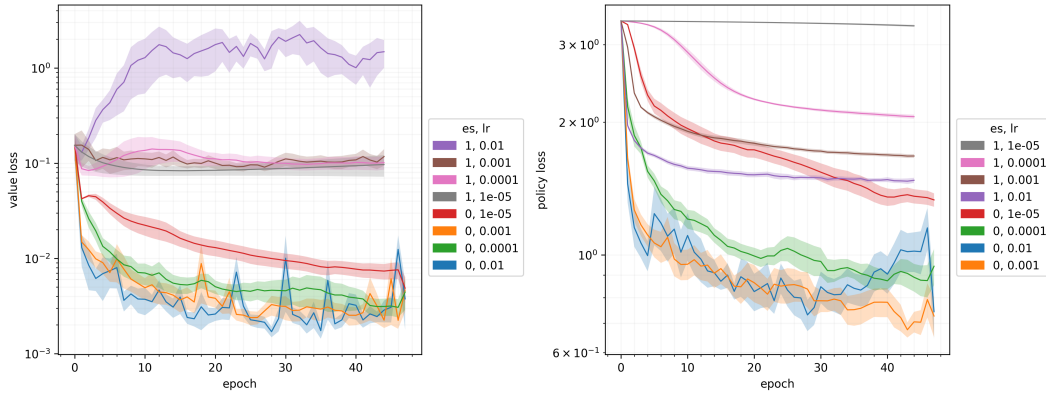


Figure 11: MDP losses.

918 **B ADDITIONAL RELATED WORK**
919
920
921922 In this section, we include additional related work that did not fit in the body of the paper.
923
924925 **B.1 AGENTS THAT USE NEURAL NETWORKS AND PLANNING**
926927 *Value Iteration Network (VIN)* (Tamar et al., 2016) is a fully differentiable network with a planning
928 module embedded within. It can learn to plan and predict outcomes that involve planning-based
929 reasoning, such as policies for reinforcement learning. It uses a differentiable approximation of
930 the value-iteration algorithm, which can be represented as a convolutional network, and is trained
931 end-to-end using standard backpropagation.932 Predictron (Silver et al., 2017b) consists of a fully abstract model, represented by a Markov reward
933 process, that can be rolled forward multiple “imagined” planning steps. Each forward pass accumulates
934 internal rewards and values over multiple planning depths. The model is trained end-to-end so
935 as to make these accumulated values accurately approximate the true value function.936 *Value Prediction Network (VPN)* (Oh et al., 2017) integrates model-free and model-based RL methods
937 into a single network. In contrast to previous model-based methods, it learns a dynamics model
938 with abstract states that is trained to make action-conditional predictions of future returns rather than
939 future observations. VIN performs value iteration over the entire state space, which requires that 1)
940 the state space is small and representable as a vector with each dimension corresponding to a separate
941 state and 2) the states have a topology with local transition dynamics (such as a 2D grid). VPN does
942 not have these limitations. VPN is trained to make its predicted values, rewards, and discounts match
943 up with those of the real environment (Oh et al., 2017, §3.3).944 *Imagination-Augmented Agent (I2A)* (Racanière et al., 2017) augments a model-free agent with
945 imagination by using environment models to simulate imagined trajectories, which are provided as
946 additional context to a policy network. An environment model is any recurrent architecture which can
947 be trained in an unsupervised fashion from agent trajectories. Given a past state and current action,
948 the environment model predicts the next state and observation. The imagined trajectory is initialized
949 with the current observation and rolled out multiple time steps into the future by feeding simulated
950 observations.951 MCTSnet (Guez et al., 2018) incorporates simulation-based search inside a neural network, by
952 expanding, evaluating and backing-up a vector embedding. The parameters of the network are trained
953 end-to-end using gradient-based optimization. When applied to small searches in the well-known
954 planning problem Sokoban, it outperformed prior MCTS baselines.955 TreeQN (Farquhar et al., 2018) is an end-to-end differentiable architecture that substitutes value
956 function networks in discrete-action domains. Instead of directly estimating the state-action value
957 from the current encoded state, as in *Deep Q-Networks (DQN)* (Mnih et al., 2015), it uses a learned
958 dynamics model to perform planning up to some fixed-depth. The result is a recursive, tree-structured
959 network between the encoded state and the predicted state-action values at the leafs. The authors
960 also propose ATreeC, an actor-critic variant that augments TreeQN with a softmax layer to form a
961 stochastic policy network. Unlike MCTS-based methods, the shape of the planning tree is fixed, and
962 the agent cannot “focus” on more promising subtrees to expand during planning.963 Yang et al. (2020) proposed Continuous MuZero, an extension of MuZero to continuous actions,
964 and showed that it outperforms the *soft actor-critic (SAC)* algorithm. Hubert et al. (2021) proposed
965 Sampled MuZero, an extension of the MuZero algorithm that is able to learn in domains with
966 arbitrarily complex action spaces (including ones that are continuous and high-dimensional) by
967 planning over sampled actions.968 Stochastic MuZero (Antonoglou et al., 2022) extended MuZero to environments that are inherently
969 stochastic, partially observed, or so large and complex that they appear stochastic to a finite agent.
970 It learns a stochastic model incorporating after-states following an action, and uses this model to
971 perform a stochastic tree search. It matches or exceeds the state of the art in a canonical set of
972 environments, including 2048.

972 B.2 MACHINE LEARNING FOR TUNING INTEGER PROGRAMMING AND COMBINATORIAL
973 OPTIMIZATION SOLVERS
974975
976 Another, different, form of learning in search techniques is tuning *integer programming (IP)* and
977 *combinatorial optimization (CO)* (Schrijver, 2003) techniques. The idea of automated algorithm
978 tuning goes back at least to Rice (1976). It has been applied in industrial practice at least since
979 2001, when Sandholm (2013) started using machine learning to learn IP algorithm configurations
980 (related to branching, cutting plane generation, *etc.*) and IP formulations based on problem instance
981 features, in the context of combinatorial auction winner determination in large-scale sourcing auctions.
982 In 2007, the leading commercial general-purpose IP solvers started shipping with such automated
983 configuration tools.
984985 IP solvers typically use a tree search algorithm called branch-and-cut. However, such solvers typically
986 come with a variety of tunable parameters that are challenging to tune by hand. Research has
987 demonstrated the power of using a data-driven approach to automatically optimize these parameters.
988989 Similarly, real-world applications that can be formulated as CO problems often have recurring patterns
990 or structure that can be exploited by heuristics. The design of good heuristics or approximation
991 algorithms for NP-hard CO problems often requires significant specialized knowledge and trial-and-
992 error, which can be a challenging and tedious process.
993994 The rest of this section reviews some of the newer work on automated algorithm configuration in IP
995 and CO.
996997 Khalil et al. (2017) sought to automate the CO tuning process using a combination of reinforcement
998 learning and graph embedding. They applied their framework to a diverse range of optimization
999 problems over graphs, learning effective algorithms for the Minimum Vertex Cover, Maximum Cut
1000 and Traveling Salesman problems.
10011002 Bengio et al. (2021) surveyed recent attempts from the machine learning and operations research
1003 communities to leverage machine learning to solve IP and CO problems. According to the authors,
1004 “Given the hard nature of these problems, state-of-the-art algorithms rely on handcrafted heuristics
1005 for making decisions that are otherwise too expensive to compute or mathematically not well defined.
1006 Thus, machine learning looks like a natural candidate to make such decisions in a more principled
1007 and optimized way.” They cite Larsen et al. (2018), who train a neural network to predict the solution
1008 of a stochastic load planning problem for which a deterministic mixed integer linear programming
1009 formulation exists. The authors state that “The nature of the application requires to output solutions
1010 in real time, which is not possible either for the stochastic version of the load planning problem or its
1011 deterministic variant when using state-of-the-art MILP solvers. Then, ML turns out to be suitable for
1012 obtaining accurate solutions with short computing times because some of the complexity is addressed
1013 offline, *i.e.*, in the learning phase, and the run-time (inference) phase is extremely quick.”
10141015 Another survey of reinforcement learning for CO can be found in Mazyavkina et al. (2021). According
1016 to the authors, “Many traditional algorithms for solving combinatorial optimization problems involve
1017 using hand-crafted heuristics that sequentially construct a solution. Such heuristics are designed by
1018 domain experts and may often be suboptimal due to the hard nature of the problems. *Reinforcement*
1019 *learning (RL)* proposes a good alternative to automate the search of these heuristics by training an
1020 agent in a supervised or self-supervised manner.”
10211022 To address the scalability challenge in large-scale CO, Qiu et al. (2022) propose an approach called
1023 *Differentiable Meta Solver (DIMES)*. Unlike previous deep reinforcement learning methods, which
1024 suffer from costly autoregressive decoding or iterative refinements of discrete solutions, DIMES
1025 introduces a compact continuous space for parameterizing the underlying distribution of candidate
solutions. Such a continuous space allows stable REINFORCE-based training and fine-tuning via
massively parallel sampling.
10261027 Aironi et al. (2024) proposed a graph-based neural approach to linear sum assignment problems,
1028 which are well-known CO problems with applications in domains such as logistics, robotics, and
1029 telecommunications. In general, obtaining an optimal solution to such problems is computationally
1030 infeasible even in small settings, so heuristic algorithms are often used to find near-optimal solutions.
1031 Their paper investigated a general-purpose learning strategy that uses a bipartite graph to describe the
1032 problem structure and a message-passing graph neural network model to learn the correct mapping.
1033

1026 The proposed graph-based solver, although sub-optimal, exhibited the highest scalability, compared
 1027 with other state-of-the-art heuristic approaches.

1028 Georgiev et al. (2024) note that “Solving NP-hard/complete combinatorial problems with neural
 1029 networks is a challenging research area that aims to surpass classical approximate algorithms. The
 1030 long-term objective is to outperform hand-designed heuristics for NP-hard/complete problems by
 1031 learning to generate superior solutions solely from training data.” The authors proposed leveraging
 1032 recent advancements in neural algorithmic reasoning to improve learning of CO problems.

1033 Balcan et al. (2024) provide the first sample complexity guarantees for tree search parameter tuning,
 1034 bounding the number of samples sufficient to ensure that the average performance of tree search over
 1035 the samples nearly matches its future expected performance on the unknown instance distribution.
 1036 Balcan et al. (2021) prove the first guarantees for learning high-performing cut-selection policies
 1037 tailored to the instance distribution at hand using samples. Balcan et al. (2022) derive sample
 1038 complexity guarantees for using machine learning to determine which cutting planes to apply during
 1039 branch-and-cut.

C STATISTICAL TESTS

1041 We show statistical tests for each environment in Table 1. For each environment’s comparison, we
 1042 selected the best-performing learning rate for each method (AlphaZero vs. AlphaZeroES) under 10
 1043 trials, and compare the final mean scores. We used the same JAX PRNG key for each individual pair,
 1044 that is, common random numbers.

| Environment | Wilcoxon signed-rank test | | Paired t-test | |
|-------------|---------------------------|-------------|---------------|---------------------------|
| | statistic | p-value | statistic | p-value |
| Navigation | 55 | 0.000976562 | 24.1637 | 8.51516×10^{-10} |
| Sokoban | 55 | 0.000976562 | 24.3562 | 7.93596×10^{-10} |
| TSP | 55 | 0.000976562 | 6.89033 | 3.57182×10^{-5} |
| VKCP | 55 | 0.000976562 | 13.4227 | 1.47451×10^{-7} |
| MDP | 55 | 0.000976562 | 3.85802 | 0.00192935 |

1056 Table 1: Statistical tests for each environment.

1057 All pairwise differences were positive, so the Wilcoxon statistic maxed out at $n(n + 1)/2 =$
 1058 $10 \times 11/2 = 55$. All p-values are well under 0.05. In conclusion, all the results are highly
 1059 statistically significant.

D SCALABILITY

1060 In this section, we run experiments that test the scalability of our method, AlphaZeroES, in comparison
 1061 to standard AlphaZero. Specifically, we see which method performs best for various problem sizes
 1062 (such as number of nodes for TSP problems). Each individual run received exactly 1 hour of training
 1063 time on a single NVIDIA A100 SXM4 40GB GPU. Results are shown in Figures 12, 13, and 14.
 1064 In the legends of these plots, `loss=alphazero` denotes AlphaZero and `loss=score_es` denotes
 1065 AlphaZeroES. Likewise, in Figure 15, we compare the scalability of AlphaZero against AlphaZeroES
 1066 in terms of the size of the network (specifically, the hidden layer size). In all figures, AlphaZeroES
 1067 outperforms AlphaZero regardless of the scale of the problem.

1068 Regarding the performance of OpenAI-ES vs. classical gradient-based methods on high-dimensional
 1069 problems, Salimans et al. (2017) note the following: “The resemblance of ES to finite differences
 1070 suggests the method will scale poorly with the dimension of the parameters θ . [...] However, it is
 1071 important to note that this does not mean that larger neural networks will perform worse than smaller
 1072 networks when optimized using ES: **what matters is the difficulty, or intrinsic dimension, of**
 1073 **the optimization problem** [emphasis added]. To see that the dimensionality of our model can be
 1074 completely separate from the effective dimension of the optimization problem, consider a regression
 1075 problem where we approximate a univariate variable y with a linear model $\hat{y} = \mathbf{x} \cdot \mathbf{w}$: if we double
 1076 the number of features and parameters in this model by concatenating \mathbf{x} with itself (i.e. using features

1080 $\mathbf{x}' = (\mathbf{x}, \mathbf{x})$), the problem does not become more difficult. The ES algorithm will do exactly the same
1081 thing when applied to this higher dimensional problem, as long as we divide the standard deviation of
1082 the noise by two, as well as the learning rate.”
1083
1084
1085
1086
1087
1088
1089
1090
1091
1092
1093
1094
1095
1096
1097
1098
1099
1100
1101
1102
1103
1104
1105
1106
1107
1108
1109
1110
1111
1112
1113
1114
1115
1116
1117
1118
1119
1120
1121
1122
1123
1124
1125
1126
1127
1128
1129
1130
1131
1132
1133

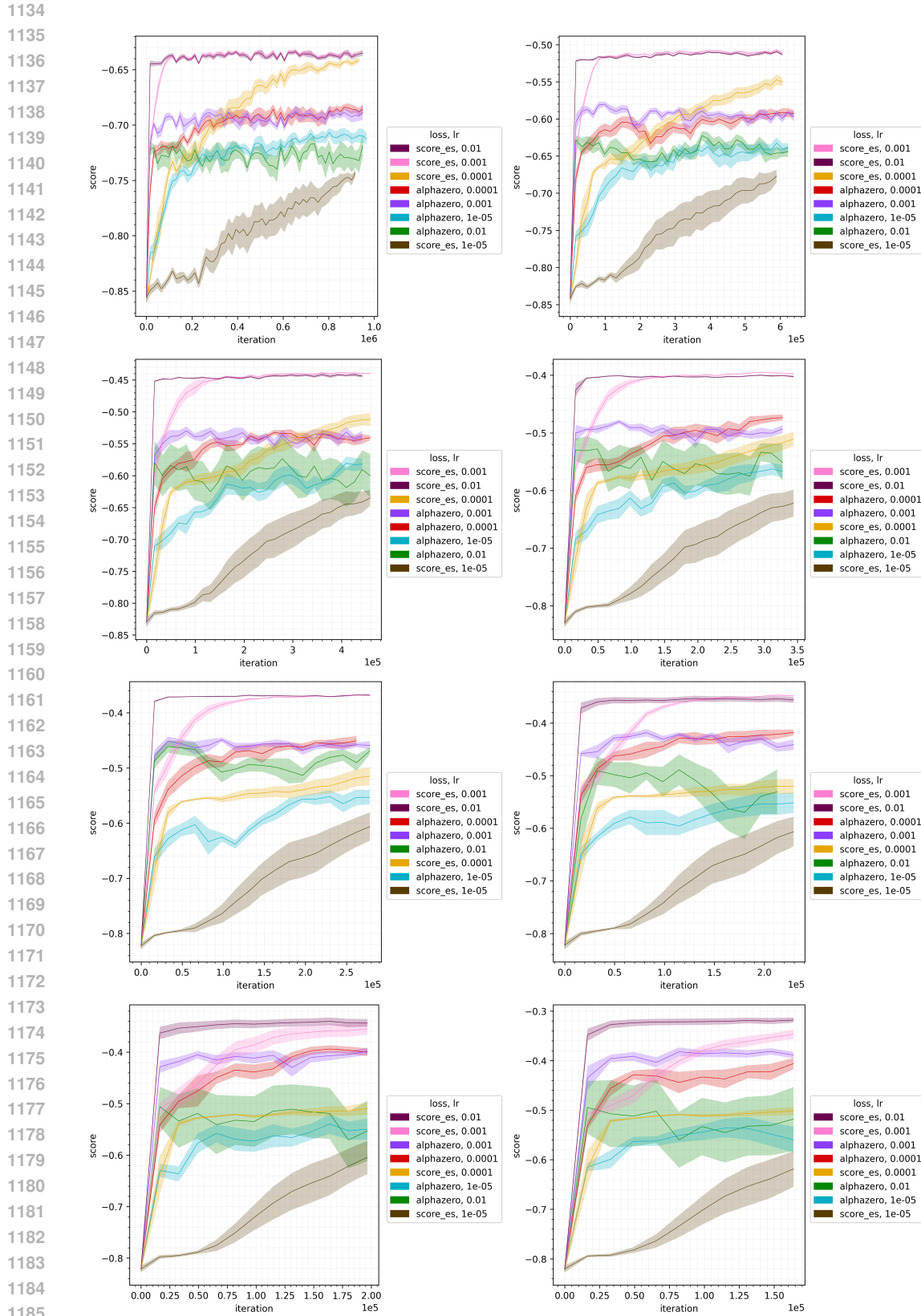


Figure 12: TSP with 8, 12, 16, 20, 24, 28, 32, and 36 points (left to right, top to bottom).

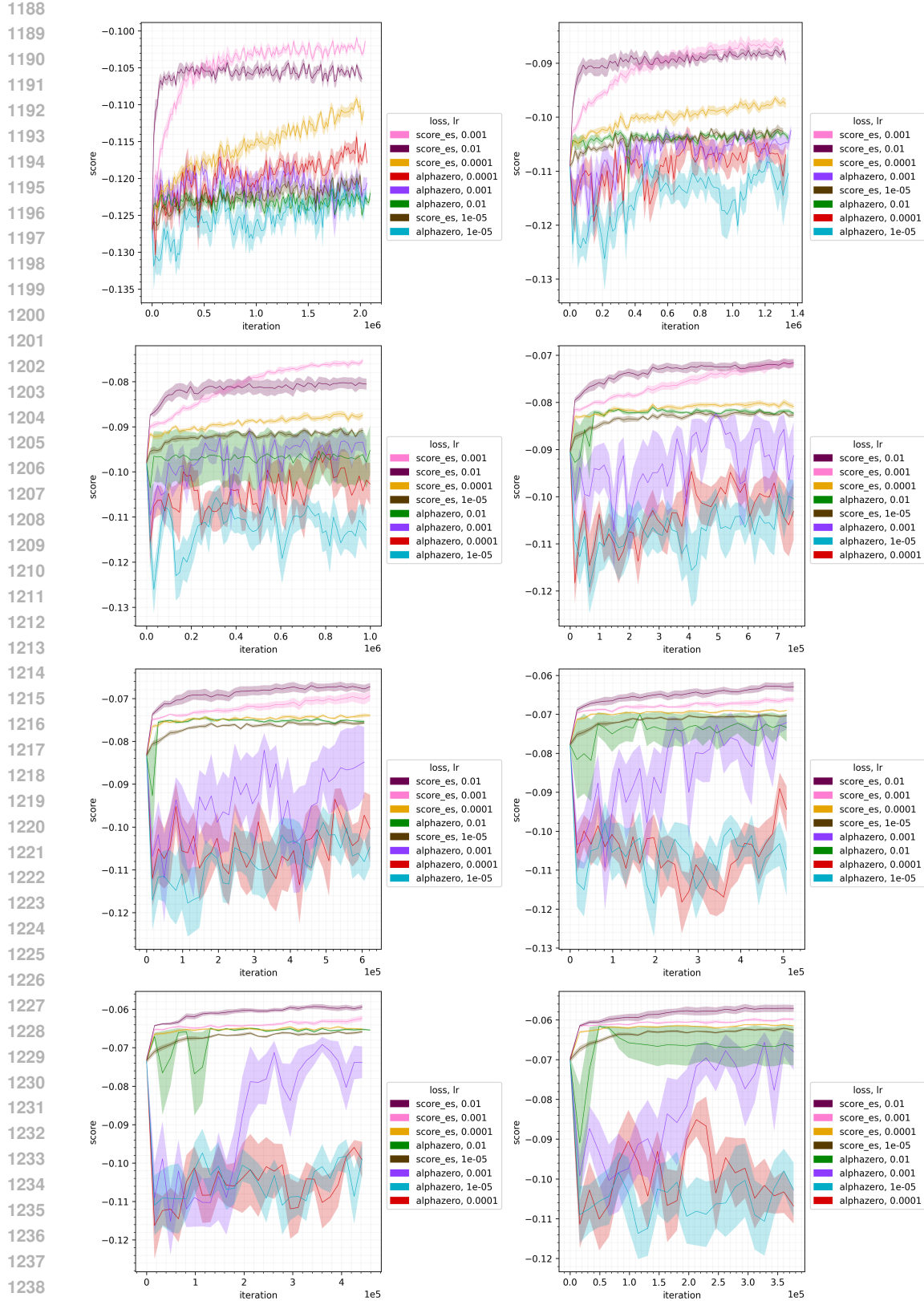
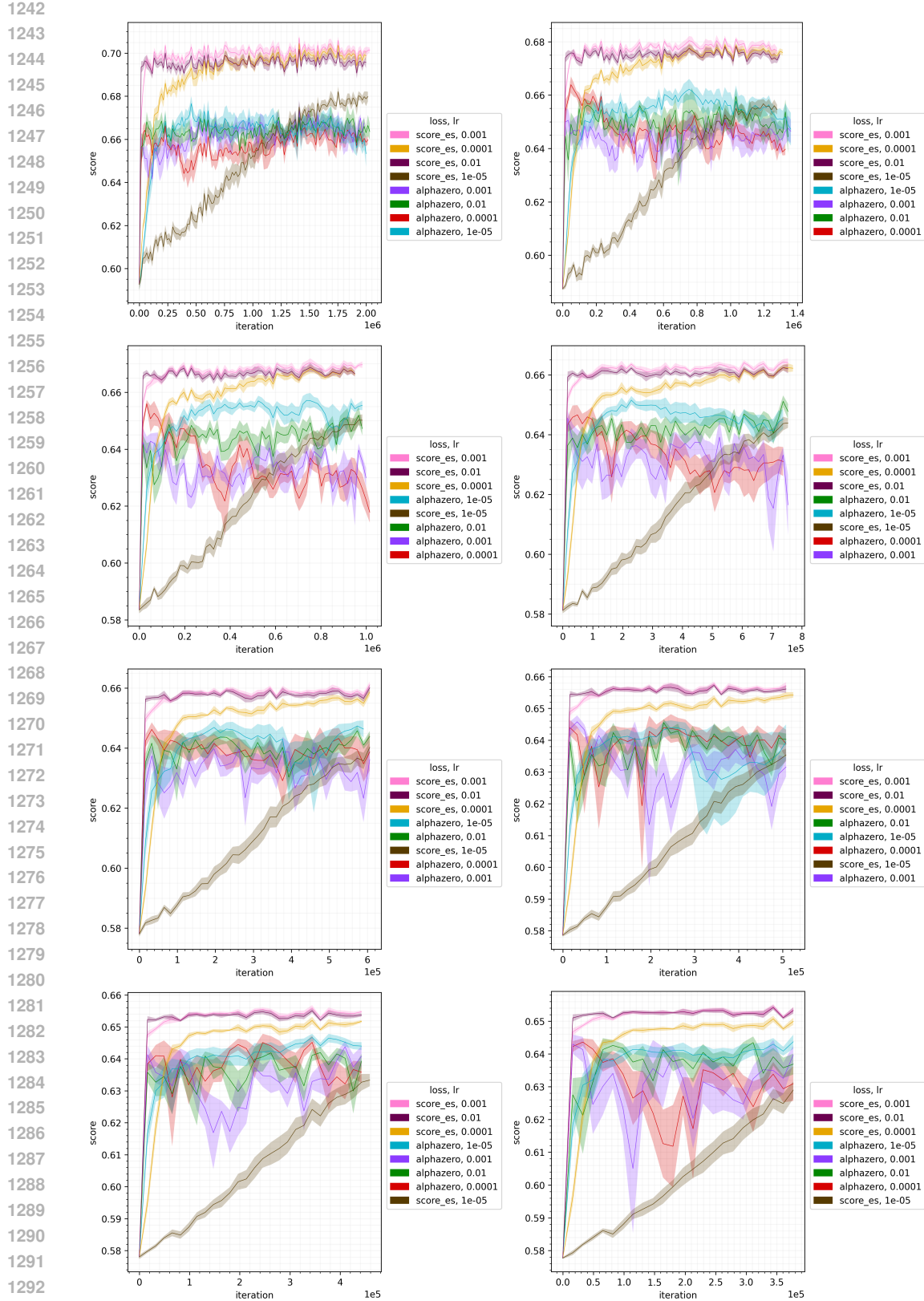


Figure 13: VKCP with 8, 12, 16, 20, 24, 28, 32, and 36 points (left to right, top to bottom). The size of the choice set is half the number of points.



1294
1295 Figure 14: MDP with 8, 12, 16, 20, 24, 28, 32, and 36 points (left to right, top to bottom). The size of
the choice set is half the number of points.

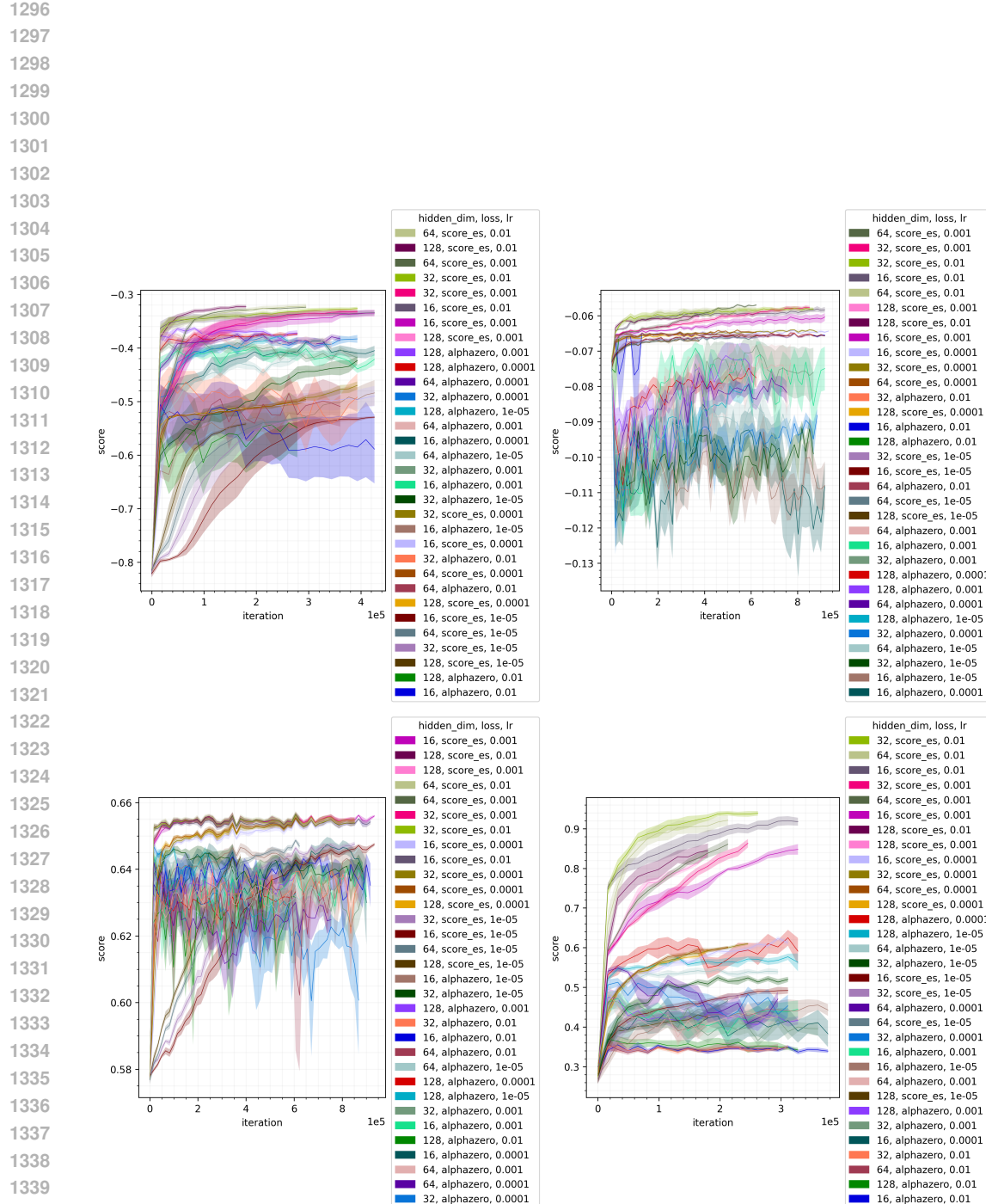


Figure 15: Performance comparison for different network sizes. Left to right, top to bottom: TSP, VKCP, MDP, and Navigation.

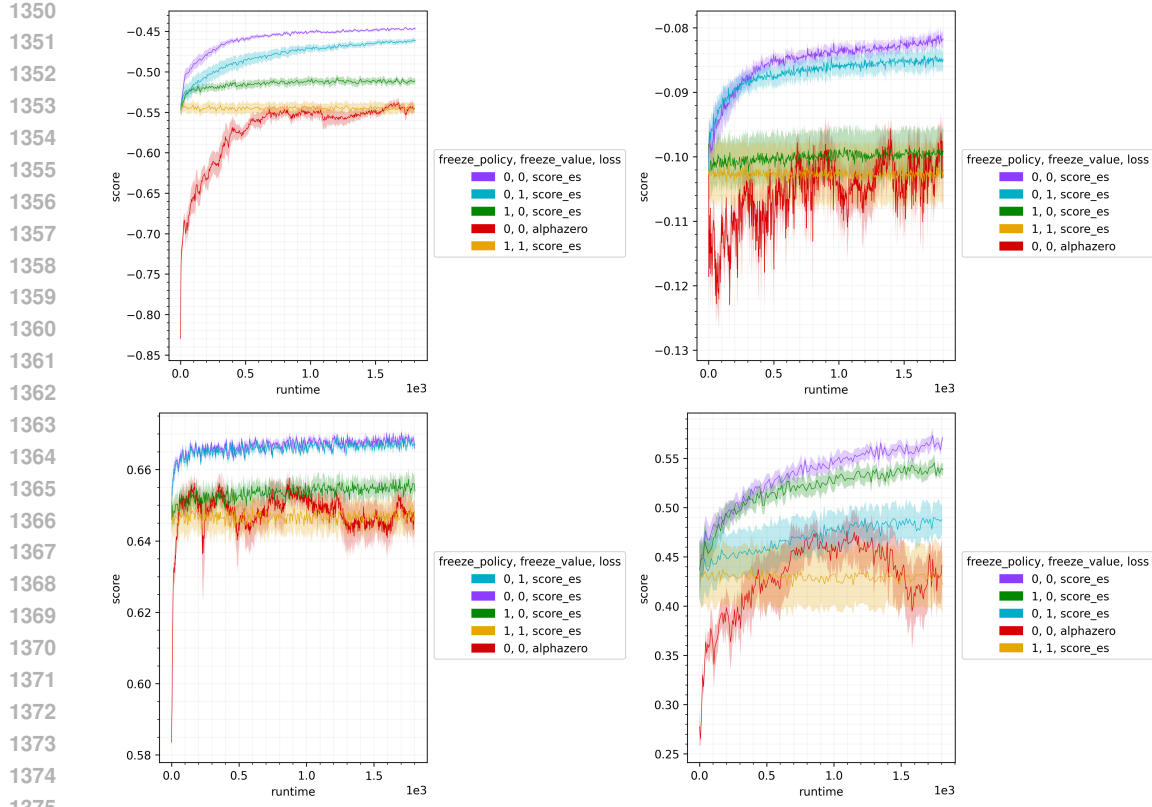


Figure 16: Ablation. Left to right, top to bottom: TSP, VKCP, MDP, and Navigation.

E ABLATION

To further investigate where the advantage of AlphaZeroES over AlphaZero comes from, and whether most of the improvement comes from a better value or policy output, we conducted an ablation study as follows. First, we train a combined policy/value network under the standard AlphaZero loss, as described in §4 and §5. Second, we create two copies of this network and use only the value output of one (henceforth, we call it the *value* network) and the policy output of the other (henceforth, we call it the *policy* network). We do this so that we can further train the value and policy outputs separately, starting from the parameters obtained by vanilla AlphaZero. Third, we *freeze* the value network (or policy network) and train *only* the policy network (or value network) under ES.

Results are shown in Figure 16. The original AlphaZero baseline is labeled with `loss=alphazero`. The subsequent training runs, which start from the final parameters of this baseline, are labeled with `loss=score_es`. The label `freeze_policy` denotes whether the policy network is frozen. The label `freeze_value` denotes whether the value network is frozen. As expected, allowing either (or both) of these to be further trained under ES improves performance over the AlphaZero baseline. Furthermore, allowing *both* of them to be trained yields maximum performance. In some environments, namely TSP, VKCP, and MDP, freezing only the value network outperforms freezing only the policy network, suggesting that improving the policy output is more important. In other environments, namely Navigation, freezing only the policy network outperforms freezing only the value network, suggesting that improving the value output is more important. Thus, interestingly, where most of the improvement of AlphaZeroES over vanilla AlphaZero comes from—a better value output or a better policy output—is environment-dependent.

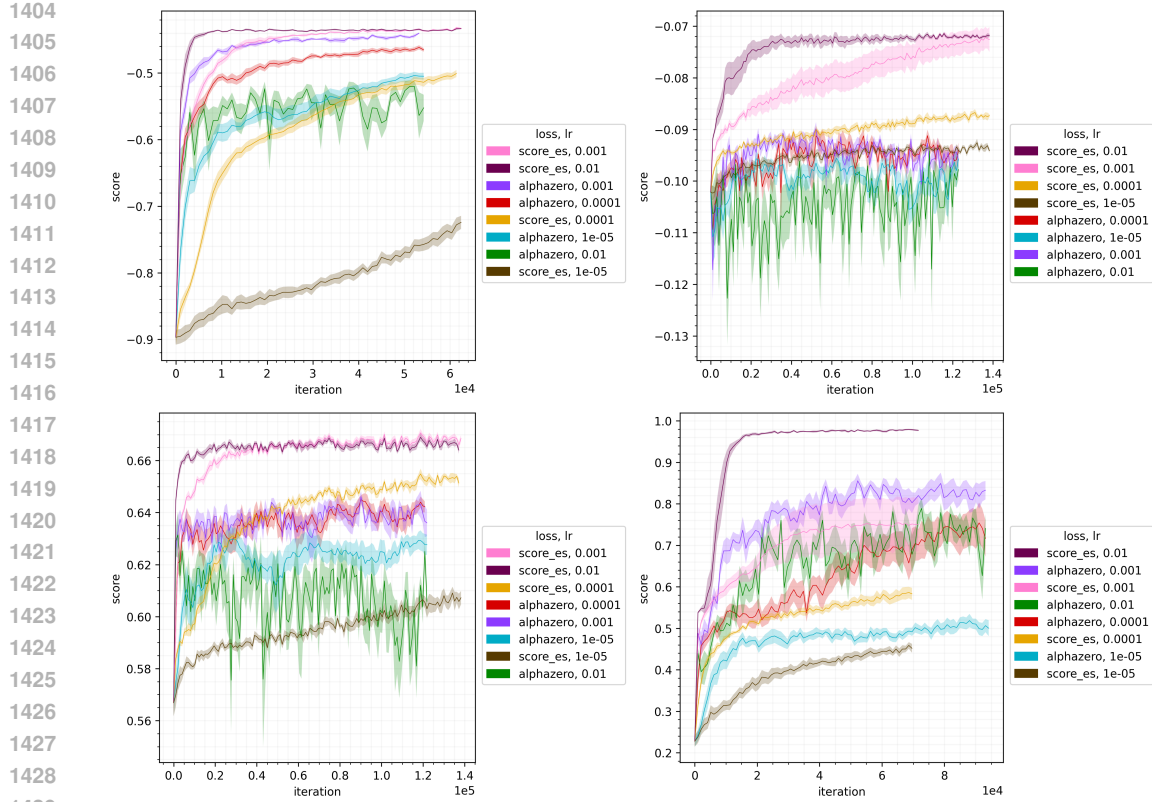


Figure 17: Performance under the attention-based architecture on TSP, VKCP, MDP, and Navigation.

F ARCHITECTURE COMPARISON

To check whether our approach generalizes to architectures rather than DeepSets (Zaheer et al., 2017), we run experiments with a different architecture, namely one based on neural attention (Vaswani et al., 2017). A theoretical comparison of these two architectures can be found in Wagstaff et al. (2022). Our architecture starts by applying an affine layer mapping the multiset of inputs to a multiset of hidden vectors. Then, we apply a sequence of D attention blocks, where D is a depth hyperparameter. (We use $D = 2$.) Each such block is a parallel attention block, as described in Zhao et al. (2019). It applies layer normalization (Ba et al., 2016), followed by a parallel application of (1) a pointwise feedforward multilayer perceptron with a single hidden layer and (2) a multi-head attention module (Vaswani et al., 2017). These two outputs are then combined with a skip connection from the input to the block, via simple addition. For reduction, we apply a many-to-one multi-head attention module on a learned readout vector initialized with random normal entries. After that, we apply the ReLU activation function followed by an affine layer. Results are shown in Figure 17. Our method, AlphaZeroES, continues to outperform AlphaZero on the new architecture.

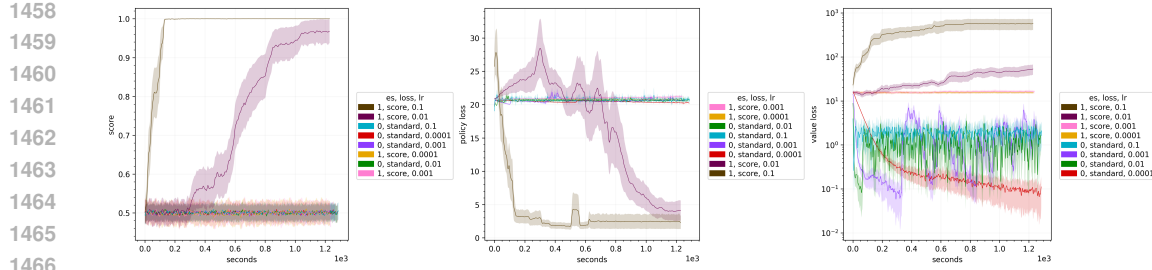


Figure 18: XOR environment metrics.

G FAILURE MODES FOR ALPHAZERO

In this section, we give concrete examples of *simple* environments where AlphaZero fails while AlphaZeroES succeeds.

G.1 XOR ENVIRONMENT

Consider the following environment. A state is a triple (b, c, t) where $b, c \in \{0, 1\}$ are bits and $t \in \mathbb{N}$ is the timestep. At the beginning of an episode, $b \in \{0, 1\}$ is sampled uniformly at random, $c = b$, and $t = 0$. An action is a bit $a \in \{0, 1\}$.

Letting a be the current action, the transition function yields $(b, c', t + 1)$, where $c' = b \oplus a$ if $t = 0$ and $c' = c$ otherwise. In other words, $c = b \oplus a_0$ for the remainder of the episode, where a_0 is the initial action. At the end of the episode, the reward is $b \oplus c = b \oplus (b \oplus a_0) = a_0$. Therefore, after the initial step, the value of state (b, c, t) is just a_0 .

Therefore, this environment has an optimal policy that is very simple: always play $a = 1$. This constant policy should be easily discoverable by optimizing episode score via ES.

Suppose that we use AlphaZero with a linear function approximator for its prediction network. At the initial timestep, MCTS inspects the two successor states $(b, b, 1)$ and $(b, b \oplus 1, 1)$, and potentially their descendants, to decide which action to play. However, with a linear function approximator, AlphaZero’s prediction network is unable to extract the key information $b \oplus c = b \oplus (b \oplus a_0) = a_0$, which determines the value of the state being examined.

Therefore, when AlphaZero is trained with the standard planning loss, it has no way to determine which action it should take at the initial timestep. (Provided that the episode is long enough that MCTS does not expand all the way to the terminal nodes.) On the other hand, AlphaZeroES can simply learn to always put all of the predicted prior probability on $a = 1$, which causes it to always be chosen by MCTS. Thus, we predict that AlphaZero consistently fails to learn any useful policy in this environment, while AlphaZeroES does.

In practice, we observe that this is the case. We set the number of timesteps to 32 and deployed each agent. We use only a linear (or more precisely, affine) layer for the AlphaZero prediction network, directly mapping the state to a value scalar and logits vector. Other hyperparameters are the same as in the rest of the experiments. Results are shown in Figure 18. As expected, AlphaZero fails to learn any useful policy, while AlphaZeroES learns the optimal policy.

G.2 ENCRYPTED ENVIRONMENT

Consider the environment. Suppose that the states of the environment are “encrypted” counters. In any state, action A decrypts the counter with a secret key, *increments* it, and re-encrypts it. In contrast, action B does nothing. At the end of an episode, the agent receives the value of the counter. The optimal policy is very simple: always choose A . But learning a good value function is nearly impossible from the perspective of the agent, given that it is unable to “decrypt” states. While this example may seem extreme, given its reliance on cryptography, it is an illustrative analogy: an environment can look “encrypted” from the perspective of an agent that is not sophisticated enough (at least at the beginning of training) to “understand” what the states mean.

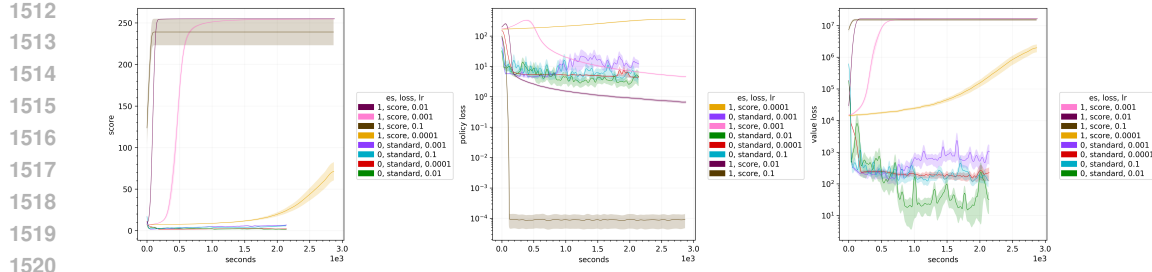


Figure 19: Encrypted environment metrics.

We implement a simple example of such an environment. For $n \in \mathbb{N}$, let $[n] = \{0, \dots, n - 1\}$. The environment’s encryption function is simply a permutation $e : [256] \rightarrow [256]$. We sample this permutation uniformly at random from the set of all permutations. Likewise, the environment’s decryption function is the inverse permutation e^{-1} .

Each state is a pair (c, t) , where $c \in [256]$ is the encrypted counter and $t \in [256]$ is the timestep. Given such a state, the agent observes the 8 bits of c , concatenated with $t/255$. The initial state is $(e(0), 0)$. Given action $a \in \{0, 1\}$, state (c, t) is mapped to $(e(e^{-1}(c) + a), t + 1)$. The environment terminates when $t = 255$, and the reward is $e^{-1}(c)$.

Results are shown in Figure 19. As expected, AlphaZeroES easily learns the trivial optimal policy, while AlphaZero struggles to learn. This is because AlphaZero essentially needs to learn a big lookup table that maps each arbitrary 8-bit pattern to an arbitrary value.

1524
1525
1526
1527
1528
1529
1530
1531
1532
1533
1534
1535
1536
1537
1538
1539
1540
1541
1542
1543
1544
1545
1546
1547
1548
1549
1550
1551
1552
1553
1554
1555
1556
1557
1558
1559
1560
1561
1562
1563
1564
1565

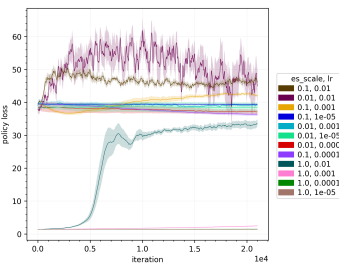
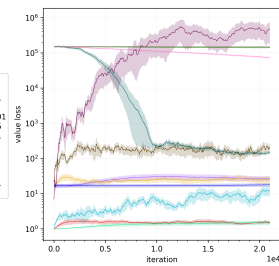
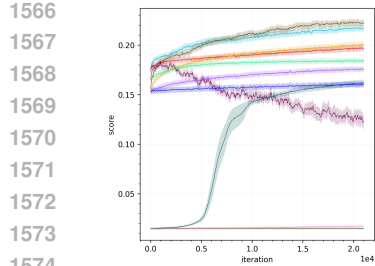


Figure 20: Sokoban.

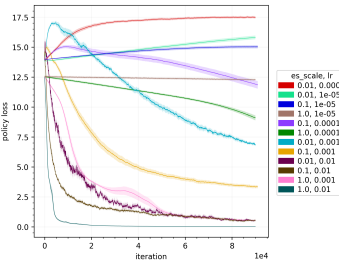
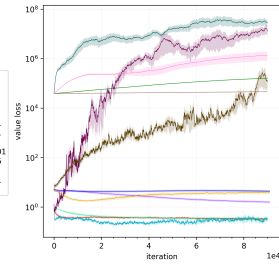
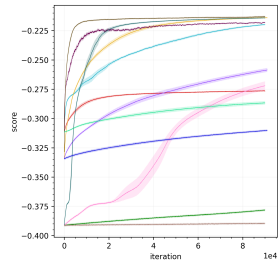


Figure 21: TSP.

H VARYING THE PERTURBATION SCALE

In this section, we explore what happens with different perturbation scales for AlphaZeroES. Results are shown in Figures 20–23. The results are qualitatively similar across different scales.

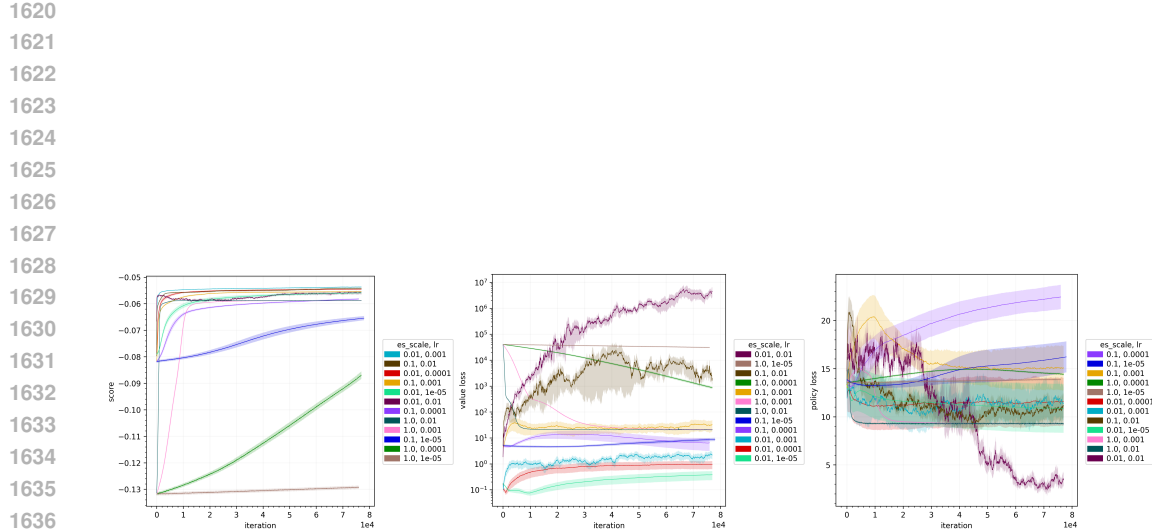


Figure 22: VKCP.

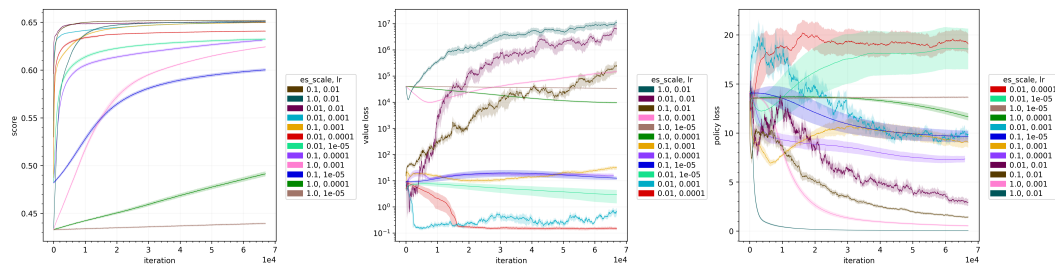


Figure 23: MDP.

I CODE

The following is an implementation of our method in the Python programming language (Van Rossum and Drake Jr., 1995). The libraries used here are described in §5 of the paper.

File rl_utils.py:

```
1680
1681 import jax
1682 from jax import lax, random
1683 from jax import numpy as jnp
1684
1685 def get_returns(episode):
1686     def f(carry, reward_discount):
1687         reward, discount = reward_discount
1688         new_carry = reward + discount * carry
1689         return new_carry, new_carry
1690
1691     rewards = episode["reward"]
1692     discounts = episode["discount"]
1693     init = jnp.zeros(rewards.shape[1:])
1694     xs = rewards, discounts
1695     _, returns = lax.scan(f, init, xs, unroll=True, reverse=True)
1696     return returns
1697
1698 def get_reach_probs(episode):
1699     discounts = episode["discount"]
1700     reach_probs = jnp.cumprod(discounts[:-1])
1701     reach_probs = jnp.insert(reach_probs, 0, 1)
1702     return reach_probs
1703
1704 def get_score(episode):
1705     reach_probs = get_reach_probs(episode)
1706     return reach_probs @ episode["reward"]
1707
1708 def sample_episode(env, agent, params, key, unroll=1):
1709     def step(state_memory, key):
1710         state, memory = state_memory
1711         action, new_memory, agent_extra = agent.apply(params, state, key,
1712             ↪ memory)
1713         reward, discount, new_state = env.step(state, action)
1714         return (new_state, new_memory), {
1715             "state": state,
1716             "action": action,
1717             "agent_extra": agent_extra,
1718             "reward": reward,
1719             "discount": discount,
1720             "memory": memory,
1721         }
1722
1723     key, subkey = random.split(key)
1724     state = env.init(subkey)
1725
1726     key, subkey = random.split(key)
1727     memory = agent.init_memory(subkey)
1728
1729     keys = random.split(key, env.max_steps())
1730     (state, memory), episode = lax.scan(step, (state, memory), keys,
1731             ↪ unroll=unroll)
1732
1733     episode["state"] = jax.tree.map(
1734         lambda xs, x: jnp.concatenate([xs, x[None]]),
```

```
1728         episode["state"],
1729         state,
1730     )
1731
1732     episode["memory"] = jax.tree.map(
1733         lambda xs, x: jnp.concatenate([xs, x[None]]),
1734         episode["memory"],
1735         memory,
1736     )
1737
1738     return episode
1739
1740     def get_num_actions(env):
1741         key = random.key(0)
1742         state = env.init(key)
1743         space = env.action_space(state)
1744         return space.mask.size
```

File rl_losses.py:

```
1746 import optax
1747 from jax import lax, nn
1748 from jax import numpy as jnp
1749
1750 from lib.rl_utils import get_reach_probs, get_returns
1751
1752 def mcts_action_loss(episode):
1753     predictions = episode["agent_extra"]["mcts_action_prediction"]
1754     targets = episode["agent_extra"]["mcts_action_target"]
1755     mask = episode["agent_extra"]["mcts_action_mask"]
1756     losses = optax.kl_divergence(
1757         nn.log_softmax(predictions, where=mask),
1758         lax.stop_gradient(targets),
1759         where=mask,
1760     )
1761     return get_reach_probs(episode) @ losses
1762
1763 def mcts_value_loss_mc(episode):
1764     """Monte Carlo."""
1765     predictions = episode["agent_extra"]["mcts_value_prediction"]
1766     targets = get_returns(episode)
1767     losses = optax.squared_error(
1768         predictions,
1769         lax.stop_gradient(targets),
1770     )
1771     return get_reach_probs(episode) @ losses
1772
1773 def mcts_value_loss_dp(episode):
1774     """Dynamic programming or self-bootstrapping."""
1775     predictions = episode["agent_extra"]["mcts_value_prediction"]
1776     targets = episode["agent_extra"]["mcts_value_target"]
1777     losses = optax.squared_error(
1778         predictions,
1779         lax.stop_gradient(targets),
1780     )
1781     return get_reach_probs(episode) @ losses
1782
1783 def alphazero_loss(episode):
1784     value_loss = mcts_value_loss_mc(episode)
```

```

1782     action_loss = mcts_action_loss(episode)          44
1783     loss = value_loss + action_loss               45
1784     metrics = {                                    46
1785         "value_loss": value_loss,                  47
1786         "action_loss": action_loss,                48
1787         "loss": loss,                           49
1788     }                                              50
1789     return loss, metrics                         51
1790
1791 def mcts_consistency_loss(episode):           52
1792     value_loss = mcts_value_loss_dp(episode)      53
1793     action_loss = mcts_action_loss(episode)       54
1794     loss = value_loss + action_loss              55
1795     metrics = {                                    56
1796         "value_loss": value_loss,                  57
1797         "action_loss": action_loss,                58
1798         "loss": loss,                           59
1799     }                                              60
1800     return loss, metrics                         61
1801
1802 File mcts.py:                                62
1803
1804
1805
1806
1807
1808
1809
1810
1811
1812
1813
1814
1815
1816
1817
1818
1819
1820
1821
1822
1823
1824
1825
1826
1827
1828
1829
1830
1831
1832
1833
1834
1835

```

```

1801 import jax
1802 import mctx
1803 from jax import lax, nn
1804 from jax import numpy as jnp
1805
1806
1807 def gumbel_muzero(
1808     state,
1809     prediction_fn,
1810     step_fn,
1811     action_mask,
1812     budget,
1813     key,
1814     algorithm="gumbel_muzero",
1815     **kwargs,
1816 ):
1817     def root_fn(state):
1818         value, logits = prediction_fn(state)
1819         return mctx.RootFnOutput(
1820             prior_logits=logits, # type: ignore
1821             value=value, # type: ignore
1822             embedding=state, # type: ignore
1823         )
1824
1825     def recurrent_fn(params, key, action, state):
1826         reward, discount, new_state = step_fn(state, action)
1827         value, logits = prediction_fn(new_state)
1828         output = mctx.RecurrentFnOutput(
1829             reward=reward, # type: ignore
1830             discount=discount, # type: ignore
1831             prior_logits=logits, # type: ignore
1832             value=value, # type: ignore
1833         )
1834         return output, new_state
1835
1836     algorithm_fn = {
1837         "gumbel_muzero": mctx.gumbel_muzero_policy,
1838         "muzero": mctx.muzero_policy,
1839     }[algorithm]
1840
1841     root = root_fn(state)
1842
1843
1844
1845
1846
1847
1848
1849
1850
1851
1852
1853
1854
1855
1856
1857
1858
1859
1860
1861
1862
1863
1864
1865
1866
1867
1868
1869
1870
1871
1872
1873
1874
1875
1876
1877
1878
1879
1880
1881
1882
1883
1884
1885
1886
1887
1888
1889
1890
1891
1892
1893
1894
1895
1896
1897
1898
1899
1900
1901
1902
1903
1904
1905
1906
1907
1908
1909
1910
1911
1912
1913
1914
1915
1916
1917
1918
1919
1920
1921
1922
1923
1924
1925
1926
1927
1928
1929
1930
1931
1932
1933
1934
1935
1936
1937
1938
1939
1940
1941
1942
1943
1944
1945
1946
1947
1948
1949
1950
1951
1952
1953
1954
1955
1956
1957
1958
1959
1960
1961
1962
1963
1964
1965
1966
1967
1968
1969
1970
1971
1972
1973
1974
1975
1976
1977
1978
1979
1980
1981
1982
1983
1984
1985
1986
1987
1988
1989
1990
1991
1992
1993
1994
1995
1996
1997
1998
1999
2000
2001
2002
2003
2004
2005
2006
2007
2008
2009
2010
2011
2012
2013
2014
2015
2016
2017
2018
2019
2020
2021
2022
2023
2024
2025
2026
2027
2028
2029
2030
2031
2032
2033
2034
2035
2036
2037
2038
2039
2040
2041
2042
2043
2044
2045
2046
2047
2048
2049
2050
2051
2052
2053
2054
2055
2056
2057
2058
2059
2060
2061
2062
2063
2064
2065
2066
2067
2068
2069
2070
2071
2072
2073
2074
2075
2076
2077
2078
2079
2080
2081
2082
2083
2084
2085
2086
2087
2088
2089
2090
2091
2092
2093
2094
2095
2096
2097
2098
2099
2100
2101
2102
2103
2104
2105
2106
2107
2108
2109
2110
2111
2112
2113
2114
2115
2116
2117
2118
2119
2120
2121
2122
2123
2124
2125
2126
2127
2128
2129
2130
2131
2132
2133
2134
2135
2136
2137
2138
2139
2140
2141
2142
2143
2144
2145
2146
2147
2148
2149
2150
2151
2152
2153
2154
2155
2156
2157
2158
2159
2160
2161
2162
2163
2164
2165
2166
2167
2168
2169
2170
2171
2172
2173
2174
2175
2176
2177
2178
2179
2180
2181
2182
2183
2184
2185
2186
2187
2188
2189
2190
2191
2192
2193
2194
2195
2196
2197
2198
2199
2200
2201
2202
2203
2204
2205
2206
2207
2208
2209
2210
2211
2212
2213
2214
2215
2216
2217
2218
2219
2220
2221
2222
2223
2224
2225
2226
2227
2228
2229
2230
2231
2232
2233
2234
2235
2236
2237
2238
2239
2240
2241
2242
2243
2244
2245
2246
2247
2248
2249
2250
2251
2252
2253
2254
2255
2256
2257
2258
2259
2260
2261
2262
2263
2264
2265
2266
2267
2268
2269
2270
2271
2272
2273
2274
2275
2276
2277
2278
2279
2280
2281
2282
2283
2284
2285
2286
2287
2288
2289
2290
2291
2292
2293
2294
2295
2296
2297
2298
2299
2300
2301
2302
2303
2304
2305
2306
2307
2308
2309
2310
2311
2312
2313
2314
2315
2316
2317
2318
2319
2320
2321
2322
2323
2324
2325
2326
2327
2328
2329
2330
2331
2332
2333
2334
2335
2336
2337
2338
2339
2340
2341
2342
2343
2344
2345
2346
2347
2348
2349
2350
2351
2352
2353
2354
2355
2356
2357
2358
2359
2360
2361
2362
2363
2364
2365
2366
2367
2368
2369
2370
2371
2372
2373
2374
2375
2376
2377
2378
2379
2380
2381
2382
2383
2384
2385
2386
2387
2388
2389
2390
2391
2392
2393
2394
2395
2396
2397
2398
2399
2400
2401
2402
2403
2404
2405
2406
2407
2408
2409
2410
2411
2412
2413
2414
2415
2416
2417
2418
2419
2420
2421
2422
2423
2424
2425
2426
2427
2428
2429
2430
2431
2432
2433
2434
2435
2436
2437
2438
2439
2440
2441
2442
2443
2444
2445
2446
2447
2448
2449
2450
2451
2452
2453
2454
2455
2456
2457
2458
2459
2460
2461
2462
2463
2464
2465
2466
2467
2468
2469
2470
2471
2472
2473
2474
2475
2476
2477
2478
2479
2480
2481
2482
2483
2484
2485
2486
2487
2488
2489
2490
2491
2492
2493
2494
2495
2496
2497
2498
2499
2500
2501
2502
2503
2504
2505
2506
2507
2508
2509
2510
2511
2512
2513
2514
2515
2516
2517
2518
2519
2520
2521
2522
2523
2524
2525
2526
2527
2528
2529
2530
2531
2532
2533
2534
2535
2536
2537
2538
2539
2540
2541
2542
2543
2544
2545
2546
2547
2548
2549
2550
2551
2552
2553
2554
2555
2556
2557
2558
2559
2560
2561
2562
2563
2564
2565
2566
2567
2568
2569
2570
2571
2572
2573
2574
2575
2576
2577
2578
2579
2580
2581
2582
2583
2584
2585
2586
2587
2588
2589
2590
2591
2592
2593
2594
2595
2596
2597
2598
2599
2600
2601
2602
2603
2604
2605
2606
2607
2608
2609
2610
2611
2612
2613
2614
2615
2616
2617
2618
2619
2620
2621
2622
2623
2624
2625
2626
2627
2628
2629
2630
2631
2632
2633
2634
2635
2636
2637
2638
2639
2640
2641
2642
2643
2644
2645
2646
2647
2648
2649
2650
2651
2652
2653
2654
2655
2656
2657
2658
2659
2660
2661
2662
2663
2664
2665
2666
2667
2668
2669
2670
2671
2672
2673
2674
2675
2676
2677
2678
2679
2680
2681
2682
2683
2684
2685
2686
2687
2688
2689
2690
2691
2692
2693
2694
2695
2696
2697
2698
2699
2700
2701
2702
2703
2704
2705
2706
2707
2708
2709
2710
2711
2712
2713
2714
2715
2716
2717
2718
2719
2720
2721
2722
2723
2724
2725
2726
2727
2728
2729
2730
2731
2732
2733
2734
2735
2736
2737
2738
2739
2740
2741
2742
2743
2744
2745
2746
2747
2748
2749
2750
2751
2752
2753
2754
2755
2756
2757
2758
2759
2760
2761
2762
2763
2764
2765
2766
2767
2768
2769
2770
2771
2772
2773
2774
2775
2776
2777
2778
2779
2780
2781
2782
2783
2784
2785
2786
2787
2788
2789
2790
2791
2792
2793
2794
2795
2796
2797
2798
2799
2800
2801
2802
2803
2804
2805
2806
2807
2808
2809
2810
2811
2812
2813
2814
2815
2816
2817
2818
2819
2820
2821
2822
2823
2824
2825
2826
2827
2828
2829
2830
2831
2832
2833
2834
2835
2836
2837
2838
2839
2840
2841
2842
2843
2844
2845
2846
2847
2848
2849
2850
2851
2852
2853
2854
2855
2856
2857
2858
2859
2860
2861
2862
2863
2864
2865
2866
2867
2868
2869
2870
2871
2872
2873
2874
2875
2876
2877
2878
2879
2880
2881
2882
2883
2884
2885
2886
2887
2888
2889
2890
2891
2892
2893
2894
2895
2896
2897
2898
2899
2900
2901
2902
2903
2904
2905
2906
2907
2908
2909
2910
2911
2912
2913
2914
2915
2916
2917
2918
2919
2920
2921
2922
2923
2924
2925
2926
2927
2928
2929
2930
2931
2932
2933
2934
2935
2936
2937
2938
2939
2940
2941
2942
2943
2944
2945
2946
2947
2948
2949
2950
2951
2952
2953
2954
2955
2956
2957
2958
2959
2960
2961
2962
2963
2964
2965
2966
2967
2968
2969
2970
2971
2972
2973
2974
2975
2976
2977
2978
2979
2980
2981
2982
2983
2984
2985
2986
2987
2988
2989
2990
2991
2992
2993
2994
2995
2996
2997
2998
2999
3000
3001
3002
3003
3004
3005
3006
3007
3008
3009
3010
3011
3012
3013
3014
3015
3016
3017
3018
3019
3020
3021
3022
3023
3024
3025
3026
3027
3028
3029
3030
3031
3032
3033
3034
3035
3036
3037
3038
3039
3040
3041
3042
3043
3044
3045
3046
3047
3048
3049
3050
3051
3052
3053
3054
3055
3056
3057
3058
3059
3060
3061
3062
3063
3064
3065
3066
3067
3068
3069
3070
3071
3072
3073
3074
3075
3076
3077
3078
3079
3080
3081
3082
3083
3084
3085
3086
3087
3088
3089
3090
3091
3092
3093
3094
3095
3096
3097
3098
3099
3100
3101
3102
3103
3104
3105
3106
3107
3108
3109
3110
3111
3112
3113
3114
3115
3116
3117
3118
3119
3120
3121
3122
3123
3124
3125
3126
3127
3128
3129
3130
3131
3132
3133
3134
3135
3136
3137
3138
3139
3140
3141
3142
3143
3144
3145
3146
3147
3148
3149
3150
3151
3152
3153
3154
3155
3156
3157
3158
3159
3160
3161
3162
3163
3164
3165
3166
3167
3168
3169
3170
3171
3172
3173
3174
3175
3176
3177
3178
3179
3180
3181
3182
3183
3184
3185
3186
3187
3188
3189
3190
3191
3192
3193
3194
3195
3196
3197
3198
3199
3200
3201
3202
3203
3204
3205
3206
3207
3208
3209
3210
3211
3212
3213
3214
3215
3216
3217
3218
3219
3220
3221
3222
3223
3224
3225
3226
3227
3228
3229
3230
3231
3232
3233
3234
3235
3236
3237
3238
3239
3240
3241
3242
3243
3244
3245
3246
3247
3248
3249
3250
3251
3252
3253
3254
3255
3256
3257
3258
3259
3260
3261
3262
3263
3264
3265
3266
3267
3268
3269
3270
3271
3272
3273
3274
3275
3276
3277
3278
3279
3280
3281
3282
3283
3284
3285
3286
3287
3288
3289
3290
3291
3292
3293
3294
3295
3296
3297
3298
3299
3300
3301
3302
3303
3304
3305
3306
3307
3308
3309
3310
3311
3312
3313
3314
3315
3316
3317
3318
3319
3320
3321
3322
3323
3324
3325
3326
3327
3328
3329
3330
3331
3332
3333
3334
3335
3336
3337
3338
3339
3340
3341
3342
3343
3344
3345
3346
3347
3348
3349
3350
3351
3352
3353
3354
3355
3356
3357
3358
3359
3360
3361
3362
3363
3364
3365
3366
3367
3368
3369
3370
3371
3372
3373
3374
3375
3376
3377
3378
3379
3380
3381
3382
3383
3384
3385
3386
3387
3388
3389
3390
3391
3392
3393
3394
3395
3396
3397
3398
3399
3400
3401
3402
3403
3404
3405
3406
3407
3408
3409
3410
3411
3412
3413
3414
3415
3416
3417
3418
3419
3420
3421
3422
3423
3424
3425
3426
3427
3428
3429
3430
3431
3432
3433
3434
3435
3436
3437
3438
3439
3440
3441
3442
3443
3444
3445
3446
3447
3448
3449
3450
3451
3452
3453
3454
3455
3456
3457
3458
3459
3460
3461
3462
3463
3464
3465
3466
3467
3468
3469
3470
3471
3472
3473
3474
3475
3476
3477
3478
3479
3480
3481
3482
3483
3484
3485
3486
3487
3488
3489
3490
3491
3492
3493
3494
3495
3496
3497
3498
3499
3500
3501
3502
3503
3504
3505
3506
3507
3508
3509
3510
3511
3512
3513
3514
3515
3516
3517
3518
3519
3520
3521
3522
3523
3524
3525
3526
3527
3528
3529
3530
3531
3532
3533
3534
3535
3536
3537
3538
3539
3540
3541
3542
3543
3544
3545
3546
3547
3548
3549
3550
3551
3552
3553
3554
3555
3556
3557
3558
3559
3560
3561
3562
3563
3564
3565
3566
3567
3568
3569
3570
3571
3572
3573
3574
3575
3576
3577
3578
3579
3580
3581
3582
3583
3584
3585
3586
3587
3588
3589
3590
3591
3592
3593
3594
3595
3596
3597
3598
3599
3600
3601
3602
3603
3604
3605
3606
3607
3608
3609
3610
3611
3612
3613
3614
3615
3616
3617
3618
3619
3620
3621
3622
3623
3624
3625
3626
3627
3628
3629
3630
3631
3632
3633
3634
3635
3636
3637
3638
3639
3640
3641
3642
3643
3644
3645
3646
3647
3648
3649
3650
3651
3652
3653
3654
3655
3656
3657
3658
3659
3660
3661
3662
3663
3664
3665
3666
3667
3668
3669
3670
3671
3672
3673
3674
3675
3676
3677
3678
3679
3680
3681
3682
3683
3684
3685
3686
3687
3688
3689
3690
3691
3692
3693
3694
3695
3696
3697
3698
3699
3700
3701
3702
3703
3704
3705
3706
3707
3708
3709
3710
3711
3712
3713
3714
3715
3716
3717
3718
3719
3720
3721
3722
3723
3724
3725
3726
3727
3728
3729
3730
3731
3732
3733
3734
3735
3736
3737
3738
3739
3740
3741
3742
3743
3744
3745
3746
3747
3748
3749
3750
3751
3752
3753
3754
3755
3756
3757
3758
3759
3760
3761
3762
3763
3764
3765
3766
3767
3768
3769
3770
3771
3772
3773
3774
3775
3776
3777
3778
3779
3780
3781
3782
3783
3784
3785
3786
3787
3788
3789
3790
3791
3792
3793
3794
3795
3796
3797
3798
3799
3800
3801
3802
3803
3804
3805
3806
3807
3808
3809
3810
3811
3812
3813
3814
3815
3816
3817
3818
3819
3820
3821
3822
3823
3824
3825
3826
3827
3828
3829
3830
3831
3832
3833
3834
3835
3836
3837
3838
3839
3840
3841
3842
3843
3844
3845
3846
3847
3848
3849
3850
3851
3852
3853
3854
3855
3856
3857
3858
3859
3860
3861
3862
3863
3864
3865
3866
3867
3868
3869
3870
3871
3872
3873
3874
3875
3876
3877
3878
3879
3880
3881
3882
3883
3884
3885
3886
3887
3888
3889
3890
3891
3892
3893
3894
3895
3896
3897
3898
3899
3900
3901
3902
3903
3904
3905
3906
3907
3908
3909
3910
3911
3912
3913
3914
3915
3916
```

```

1836     outputs = algorithm_fn(
1837         params=(),
1838         rng_key=key,
1839         root=jax.tree.map(lambda x: jnp.expand_dims(x, 0), root),
1840         recurrent_fn=jax.vmap(recurrent_fn, [None, None, 0, 0]),
1841         num_simulations=budget + 1,
1842         invalid_actions=jax.tree.map(lambda x: jnp.expand_dims(~x, 0),
1843             ↪ action_mask),
1844         **kwargs,
1845     )
1846     summary = jax.tree.map(lambda x: x[0], outputs.search_tree.summary())
1847     output = jax.tree.map(lambda x: x[0], outputs)
1848     return {
1849         "action": output.action,
1850         "action_onehot": nn.one_hot(output.action, output.action_weights.
1851             ↪ size),
1852         "action_weights": lax.stop_gradient(output.action_weights),
1853         "root_value": root.value,
1854         "root_logits": root.prior_logits,
1855         "root_state": state,
1856         "search_tree": lax.stop_gradient(output.search_tree),
1857         "visit_counts": summary.visit_counts,
1858         "visit_probs": summary.visit_probs,
1859         "value": lax.stop_gradient(summary.value),
1860         "qvalues": summary.qvalues,
1861         "action_mask": action_mask,
1862     }
1863
1864
1865
1866
1867
1868
1869
1870
1871
1872
1873
1874
1875
1876
1877
1878
1879
1880
1881
1882
1883
1884
1885
1886
1887
1888
1889

```

File alphazero.py:

```

1     from functools import partial
2
3     from lib import mcts
4
5
6     class AlphaZero:
7
8         def __init__(self, env, pred_fn, budget):
9             self.env = env
10            self.pred_fn = pred_fn
11            self.budget = budget
12
13        def init(self, params_key, state, key, memory):
14            return self.pred_fn.init(params_key, state)
15
16        def init_memory(self, key):
17            return None
18
19        def apply(self, params, state, key, memory):
20            space = self.env.action_space(state)
21            output = mcts.gumbel_muzero(
22                state=state,
23                prediction_fn=partial(self.pred_fn.apply, params),
24                step_fn=self.env.step,
25                budget=self.budget,
26                key=key,
27                action_mask=space.mask,
28            )
29            return (
30                output["action"],
31                memory,
32                {
33                    "search_tree": output["search_tree"],
34                    "mcts_value_prediction": output["root_value"],
35                }
36            )
37
38
39
40
41
42
43
44
45
46
47
48
49
50
51
52
53
54
55
56
57
58
59
60
61
62
63
64
65
66

```

| | | |
|------|--|----|
| 1890 | "mcts_value_target": output["value"], | 35 |
| 1891 | "mcts_action_prediction": output["root_logits"], | 36 |
| 1892 | "mcts_action_target": output["action_weights"], | 37 |
| 1893 | "mcts_action_mask": space.mask, | 38 |
| 1894 | } | 39 |
| 1895 |) | 40 |

1896 File predictors.py:
 1897

| | | |
|------|--|----|
| 1898 | import argparse | 1 |
| 1899 | | 2 |
| 1900 | from flax import linen as nn | 3 |
| 1901 | from jax import numpy as jnp | 4 |
| 1902 | from lib import envs, rl_utils | 5 |
| 1903 | | 6 |
| 1904 | | 7 |
| 1905 | class DensePredictor(nn.Module): | 8 |
| 1906 | args: argparse.Namespace | 9 |
| 1907 | env: envs.Env | 10 |
| 1908 | | 11 |
| 1909 | @nn.compact | 12 |
| 1910 | def __call__(self, state): | 13 |
| 1911 | x = self.env.observation_vector(state) | 14 |
| 1912 | x = nn.Dense(self.args.hidden_dim)(x) | 15 |
| 1913 | x = nn.relu(x) | 16 |
| 1914 | | 17 |
| 1915 | logits = nn.Dense(rl_utils.get_num_actions(self.env))(x) | 18 |
| 1916 | | 19 |
| 1917 | if hasattr(self.env, "players"): | 20 |
| 1918 | values = nn.Dense(self.env.players)(x) | 21 |
| 1919 | return values, logits | 22 |
| 1920 | else: | 23 |
| 1921 | (value,) = nn.Dense(1)(x) | 24 |
| 1922 | return value, logits | 25 |
| 1923 | | 26 |
| 1924 | | 27 |
| 1925 | class DeepSetsPredictor(nn.Module): | 28 |
| 1926 | args: argparse.Namespace | 29 |
| 1927 | env: envs.Env | 30 |
| 1928 | | 31 |
| 1929 | @nn.compact | 32 |
| 1930 | def __call__(self, state): | 33 |
| 1931 | x, mask = self.env.observation_multiset(state) | 34 |
| 1932 | if mask is None: | 35 |
| 1933 | mask = jnp.ones(x.shape[0], bool) | 36 |
| 1934 | | 37 |
| 1935 | for _ in range(self.args.depth): | 38 |
| 1936 | x_skip = x | 39 |
| 1937 | x = nn.Dense(self.args.hidden_dim)(x) | 40 |
| 1938 | x = nn.relu(x) | 41 |
| 1939 | x1 = nn.Dense(self.args.hidden_dim)(x.sum(0, where=mask[..., | 42 |
| 1940 | ↪ None])) | 43 |
| 1941 | x1 /= 1 + mask.sum(0)[..., None] | 44 |
| 1942 | x2 = nn.Dense(self.args.hidden_dim, use_bias=False)(x) | 45 |
| 1943 | x = x1 + x2 | 46 |
| 1944 | x = nn.relu(x) | 47 |
| 1945 | if x_skip.shape == x.shape: | 48 |
| 1946 | x += x_skip | 49 |
| 1947 | | 50 |
| 1948 | match self.env: | 51 |
| 1949 | case (| 52 |
| 1950 | envs.EuclideanTSP() | 53 |
| 1951 | envs.Knapsack() | 54 |


```
1998     "readout", nn.initializers.normal(1), [self.args.hidden_dim]
1999 )
2000 x = nn.MultiHeadAttention(self.args.heads)(readout[None], x, mask
2001     ↪ =mask).squeeze(
2002         0
2003     )
2004
2005     if hasattr(self.env, "players"):
2006         values = nn.Dense(self.env.players)(x)
2007         return values, logits
2008     else:
2009         (value, ) = nn.Dense(1)(x)
2010         return value, logits
2011
2012     class MixedPredictor(nn.Module):
2013         value: nn.Module
2014         policy: nn.Module
2015
2016         @nn.compact
2017         def __call__(self, state):
2018             value, _ = self.value(state)
2019             _, logits = self.policy(state)
2020             return value, logits
```

File pseudogradient.py:

```
2021 from functools import partial
2022
2023 import jax
2024 import optax
2025 from jax import lax, random
2026 from jax import numpy as jnp
2027 from jax.scipy import stats
2028 from optax import tree_utils as otu
2029
2030 class Normal:
2031     def __init__(self, loc, scale):
2032         self.loc = loc
2033         self.scale = scale
2034
2035     def sample(self, key):
2036         z = otu.tree_random_like(key, self.loc)
2037         return jax.tree_map(lambda l, z: l + self.scale * z, self.loc, z)
2038
2039     def sample_antithetic(self, key):
2040         z = otu.tree_random_like(key, self.loc)
2041         return jax.tree_map(
2042             lambda l, z: l + self.scale * jnp.stack([z, -z]),
2043             self.loc,
2044             z,
2045         )
2046
2047     def logpdf(self, x):
2048         logpdfs = jax.tree_map(
2049             lambda l, x: stats.norm.logpdf(x, l, self.scale),
2050             self.loc,
2051             x,
2052         )
2053         return otu.tree_sum(logpdfs)
2054
2055     def smoothe(scale, distribution="normal"):
```

| | | |
|------|--|----|
| 2052 | match distribution: | 38 |
| 2053 | case "normal": | 39 |
| 2054 | distribution_cls = Normal | 40 |
| 2055 | case _: | 41 |
| 2056 | raise NotImplementedError | 42 |
| 2057 | | 43 |
| 2058 | def g(f, x, key): | 44 |
| 2059 | dist = distribution_cls(x, scale) | 45 |
| 2060 | | 46 |
| 2061 | key, subkey = random.split(key) | 47 |
| 2062 | samples = lax.stop_gradient(dist.sample_antithetic(subkey)) | 48 |
| 2063 | | 49 |
| 2064 | outputs = jax.vmap(f, [0, None], axis_size=2)(samples, key) | 50 |
| 2065 | log_probs = jax.vmap(dist.logpdf, axis_size=2)(samples) | 52 |
| 2066 | assert log_probs.ndim == 1 | 53 |
| 2067 | | 54 |
| 2068 | ones = jnp.exp(log_probs - lax.stop_gradient(log_probs)) | 55 |
| 2069 | ones /= ones.size | 56 |
| 2070 | | 57 |
| 2071 | return jax.tree.map(lambda outputs: ones @ outputs, outputs) | 58 |
| | | 59 |
| | return lambda f: partial(g, f) | 60 |
| 2072 | | |
| 2073 | | |
| 2074 | | |
| 2075 | | |
| 2076 | | |
| 2077 | | |
| 2078 | | |
| 2079 | | |
| 2080 | | |
| 2081 | | |
| 2082 | | |
| 2083 | | |
| 2084 | | |
| 2085 | | |
| 2086 | | |
| 2087 | | |
| 2088 | | |
| 2089 | | |
| 2090 | | |
| 2091 | | |
| 2092 | | |
| 2093 | | |
| 2094 | | |
| 2095 | | |
| 2096 | | |
| 2097 | | |
| 2098 | | |
| 2099 | | |
| 2100 | | |
| 2101 | | |
| 2102 | | |
| 2103 | | |
| 2104 | | |
| 2105 | | |